



Phytoplankton Composition and Environmental Drivers in the Northern Strait of Georgia (Salish Sea), British Columbia, Canada

Justin Del Bel Belluz¹ · M. Angelica Peña² · Jennifer M. Jackson¹ · Nina Nemcek²

Received: 19 March 2020 / Revised: 19 August 2020 / Accepted: 22 October 2020
© Coastal and Estuarine Research Federation 2021

Abstract

A 4-year (2015–2018) weekly to bi-weekly time series of phytoplankton biomass and composition derived from high-performance liquid chromatography (HPLC) phytoplankton pigments and Chemtax analysis is presented and used to investigate phytoplankton community dynamics at a station in the northern Strait of Georgia (NSoG). Through the time series, blooms were largely dominated by diatoms, which formed the bulk of annual biomass. Spring diatom bloom timing and magnitude varied widely and appears to have been driven by complex interactions of solar radiation, wind, stratification, and grazing. In turn, post-spring diatom blooms were mostly associated with nutrient renewal to the surface layer as suggested by redundancy analysis (RDA), which showed inverse relationships between diatoms and temperature and stratification. A single non-diatom bloom in July 2016, dominated by the silicoflagellate, *Dictyocha* sp., was the time series maximum biomass and occurred under warm, stratified conditions and a freshening of the surface layer: The Chemtax dictyochophyte group was positively linked to temperature and stratification through RDA. Outside of bloom conditions, diverse communities emerged with prasinophytes and cryptophytes showing persistent contributions and their highest biomass during summer. Uniquely, these groups often persisted through nutrient renewal and drawdown events typically associated with diatom blooms and suggestive of high grazing pressure and nutrient regeneration. The prevalence of these groups through diverse conditions likely precluded statistical links with environmental drivers. This time series is the first of its kind for the NSoG, creates a baseline for future analyses, and highlights the contributions by small species, particularly prasinophytes, to regional phytoplankton communities.

Keywords Chemtax · Phytoplankton dynamics · Environmental drivers · Pico-flagellates · Prasinophytes · Salish Sea

Introduction

Phytoplankton are responsible for nearly half of global primary production, with much of this contribution produced in coastal waters (Winder and Sommer 2012; Simo-Matchim et al. 2017). In addition to playing essential roles in climate regulation and biogeochemical cycling, phytoplankton form the base of the marine food web and provide energy to higher trophic

levels including important fisheries species (Carstensen et al. 2015; Simo-Matchim et al. 2017). Phytoplankton are composed of a diverse array of species, encompassing both prokaryotic cyanobacteria and eukaryotic algae, with many having unique ecological roles. As a result, changes in phytoplankton community composition can have wide-ranging effects on biogeochemical cycling and ecosystem function. Shifts in community composition are driven by both bottom-up forcing (physical conditions such as temperature, mixing, light availability, and nutrient inputs) and top-down forcing (grazing pressure and predator-prey interactions) (Winder and Sommer 2012). Worldwide, increasing anthropogenic pressures (i.e., nutrient loading, coastal development, and climate change) are altering how both bottom-up and top-down processes impact phytoplankton communities (Cloern and Jassby 2008; Zingone et al. 2010). In light of these changes, there is a need for improved understanding of the processes which drive phytoplankton compositions and for baseline studies that

Communicated by Hongbin Liu

✉ Justin Del Bel Belluz
justin.belluz@hakai.org

¹ Hakai Institute, Victoria, BC, Canada

² Institute of Ocean Sciences, Fisheries and Oceans Canada, Sidney, BC, Canada

investigate community composition. This information is important for marine resource management and predicting future environmental change in coastal settings.

In coastal regions, phytoplankton compositions are variable and their drivers are complex, making it difficult to discern driver-composition relationships from temporal trends (Carstensen et al. 2015). Meta-analysis of existing global time series has shown no universal phenology across ecosystems, notably at short-term and seasonal timescales, where biomass and composition can vary by orders of magnitude as a result of complex physical-environmental-grazer interactions (Zingone et al. 2010; Carstensen et al. 2015). Yet, some commonality can be found in phytoplankton composition, especially when focusing on temperate coastal regions. In these systems, blooms are predominantly composed of diatoms which constitute the bulk of annual phytoplankton biomass and provide the most efficient energy transfer to higher trophic levels, although a wide range in bloom timing, magnitude, and species occurs across systems (Muylaert et al. 2006; Goela et al. 2014; Carstensen et al. 2015). In turn, succession from diatom blooms to lower biomass conditions is often characterized by the emergence of diverse phytoplankton communities (Harrison et al. 1983). Through the employment of novel techniques (i.e., pigment analysis, genomics, and flow cytometry), it has become clear that many temperate coastal systems show periods greatly influenced, or even dominated by, nano- and pico-eukaryote species (Ansotegui et al. 2003; Not et al. 2005; Morán 2007; Foulon et al. 2008). Succession to increased contributions of these small-sized species is often ascribed to stability, nutrient limitation, temperature, or grazing (Latasa et al. 2010; Goela et al. 2014; Marañón et al. 2012). However, findings are often conflicting and drivers remain poorly understood. Further observations in temperate coastal systems could aid in developing a better understanding of both bloom and low-biomass compositional dynamics.

The Salish Sea is a large productive semi-enclosed coastal estuarine system located on the southwest coast of British Columbia, Canada, and northern Washington State, USA (Fig. 1). While the Salish Sea is geographically complex, the largest waterways are the Juan de Fuca Strait, Puget Sound, and the Strait of Georgia. The northern Strait of Georgia (NSoG), which is the focus of this study, is bounded to the south by Texada Island and to the north by Quadra Island. In the central and southern portions of the Strait of Georgia, freshwater inputs drive estuarine circulation and are largely supplied by the Fraser River, which displays a mid-June snow-ice melt-driven freshet with high discharge ($10,000 \text{ m}^3 \text{ s}^{-1}$) (Masson and Cummins 2004). Yet, the Fraser River has limited influence on the NSoG and various small streams and glacial-fed rivers, such as the Homathko River, likely have a greater influence on NSoG stratification (Masson and Peña 2009). The NSoG is connected to outer shelf waters via a complex system of narrow channels, although it is thought

that the majority of seawater exchange occurs through the southern Juan de Fuca Strait (Masson 2002; Johannessen et al. 2014). Deep water renewal occurs through this southern passage and transports high nutrients from the deep Pacific Ocean into the central basin of the Strait of Georgia (Mackas and Harrison 1997; Pawlowicz et al. 2007; Peña et al. 2016). It is these nutrients that sustain the high primary production observed in the region. Similar to the central portions of the Strait of Georgia, the NSoG experiences high spring phytoplankton biomass associated with a spring bloom (Masson and Peña 2009; Jackson et al. 2015; Suchy et al. 2019); however, in the NSoG, comparatively calmer summer winds, tidal energy, and increased stratification can lead to periods of surface layer nitrate limitation on phytoplankton growth. These periods are generally brief as wind events mix the upper water column and replenish surface nutrients (Peña et al. 2016). At times, tidal jets created by the narrow and highly turbulent northern passages can also work to inject nutrients into the surface layer of the NSoG and have been shown to create mosaicism in phytoplankton communities (Haigh and Taylor 1991; Olson et al. 2020).

There is limited knowledge of phytoplankton composition dynamics in the NSoG. For the Salish Sea and surrounding regions, historical studies have focused on the seasonal succession of spring diatom blooms to flagellate dominated communities associated with increases in stratification (Harrison et al. 1983). Similarly, a 2-year study in Sechelt Inlet (a fjord system branching off the eastern NSoG) that collected monthly phytoplankton data showed a spring diatom bloom followed by nutrient-depleted conditions dominated by flagellates including high abundances of cryptophytes and the haptophyte, *Chrysochromulina* spp. (Haigh et al. 1992). Although studies have reported harmful algal species in the NSoG (Haigh and Taylor 1990; Pawlowicz et al. 2020), we could find only a single study that examined phytoplankton community composition in our study region. In this study, novel trends were described including periods dominated by flagellates, chiefly *Chrysochromulina* spp., cryptophytes, and the pico-plankton *Micromonas pusilla*, during conditions highly favorable for diatom growth (Haigh and Taylor 1991). In addition, exceptionally high ciliate grazing rates beyond those that could be supported by nano-plankton production were observed in this study and it was hypothesized that ciliate populations were supplementing energy requirements via mixotrophy and chloroplast retention. Based on these observations, it is clear that the studied region is highly dynamic and remains poorly understood in terms of phytoplankton community dynamics.

The objectives of our work are to characterize phytoplankton community dynamics and investigate their environmental drivers at a station in the NSoG. This was done by examining a 4-year (2015–2018) time series of physical and chemical variables together with phytoplankton group composition

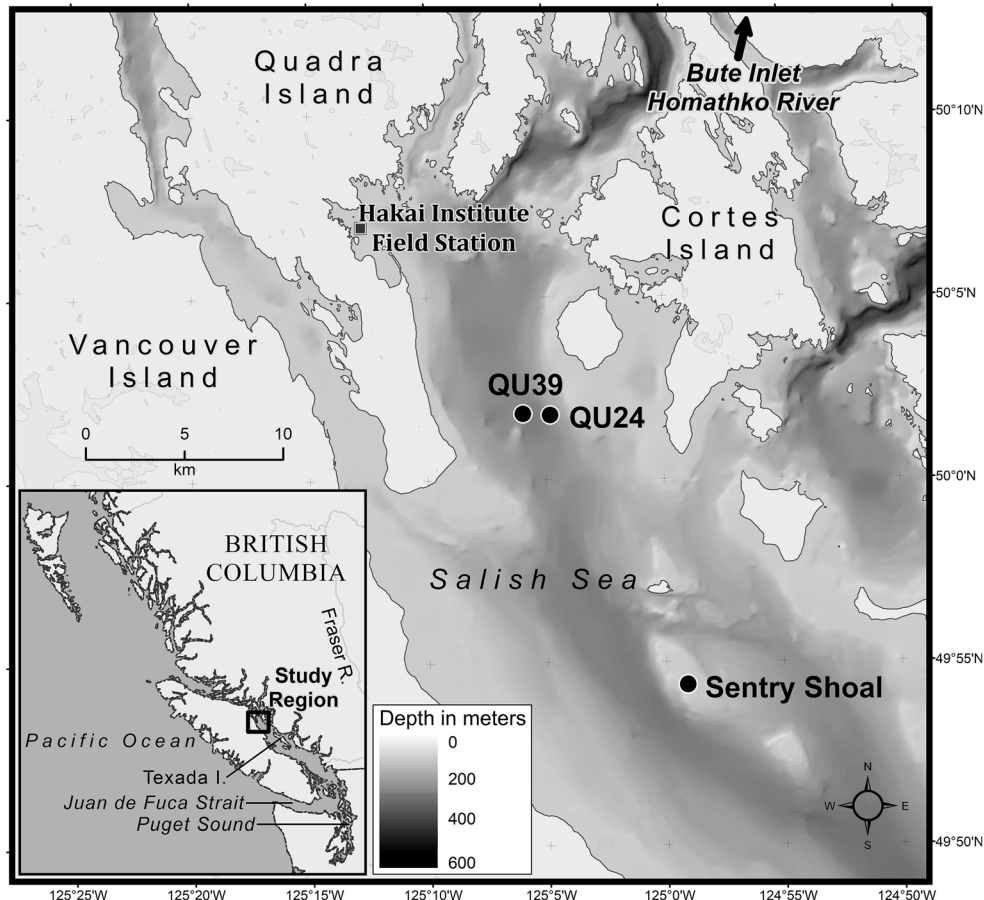


Fig. 1 Study region in the northern Strait of Georgia (NSoG) showing the location of sampling station QU24 and station QU39, the Hakai Institute field station where solar radiation data were collected, and the Environment Canada Sentry Shoal buoy (46131) where wind data were collected

derived using high-performance liquid chromatography (HPLC) pigment-based analysis and the matrix factorization program Chemtax (Mackey et al. 1996). Derivation of phytoplankton groups via Chemtax has been shown to be effective in dynamic coastal settings through its ability to characterize contributions of small pico-eukaryotic and prokaryote species not easily quantified via light microscopy (Ansotegui et al. 2003; Goela et al. 2014). Using the approach of microscopy-guided Chemtax analysis, we investigated causes of temporal variability in phytoplankton composition through comparisons with physical and chemical drivers. Although the impact of microzooplankton grazing is important (e.g., Mahara et al. 2019), it is beyond the scope of this study and will not be directly addressed. Ecologically rich, the NSoG supports a wide array of fish species including culturally and economically important Pacific salmon, herring, and hake. In the past decades, many of these species have shown declines highlighting the importance of a greater understanding of food-web dynamics for the improvement of future decision-making and conservation efforts (Beamish et al. 2010; Beamish et al. 2012).

Methods

Study Site and Sampling Regime

From 2015 through 2018, biological (chlorophyll, HPLC-derived pigments, and phytoplankton microscopy), physical (conductivity temperature depth (CTD)), and chemical (nutrients) data were collected in the NSoG at the southern edge of Sutil Channel (Fig. 1). Data were collected at station QU24 prior to March 20, 2015, and at station QU39 afterward, which was located approximately 1.3 km to the west of station QU24 (Fig. 1). The depth at both stations was approximately 260 m. For consistency, all station references will be denoted as station QU39 following this point in the text. Through the time series, data were sampled on a weekly to bi-weekly basis. In general, less data were collected during winter months and some gaps exist due to poor weather. Sampling resolution increased in the later years (2017 and 2018). CTD profiles were collected using either a Sea-Bird 19+ or RBR Maestro, and here, data from 280 CTD profiles were examined. Water samples were collected using Niskin bottles, and here, data

from primarily 5 m were examined with exception to phytoplankton microscopy samples which were collected at the subsurface (1 m depth) and used in conjunction with the 5 m depth data.

Ancillary Weather Data

Wind speed (m s^{-1}) data were collected at the Environment Canada buoy (buoy 46131) located at Sentry Shoal (Fig. 1), which is 16 km south of station QU39. Data from this buoy were assumed to be most representative of ocean conditions in the region as they were collected away from the influence of land. In the region, the surrounding mountainous terrain results in highly channelized winds along the axis of the NSoG and it is assumed that wind would have traveled over open water past both station QU39 and buoy 46131 (Bakri et al. 2017; Evans et al. 2019). For comparison, the closest terrestrial-based anemometer located at the Hakai Institute field station, 13 km northwest of station QU39, showed similar trends to buoy 46131; however, daily mean wind speeds at Hakai were often considerably less than those experienced at the buoy ($r^2 = 0.50$, $\text{Wind}_{\text{HAKAI}} = 0.29(\text{Wind}_{46131}) + 0.26$, $n = 1458$). Solar radiation (W m^{-2}) data were collected at the Hakai Institute field station as these were the closest data to station QU39. Both Sentry Shoal wind speed (1-h sampling resolution) and Hakai Institute solar radiation (5-min sampling resolution) data were converted to daily means using backwards running 4-day moving averages (-3 days + collection day). Backward moving averages were used to preserve prior wind and solar radiation values that would have influenced ocean conditions on the days field data were collected.

CTD Data

CTD data were fully processed and binned in 1-m intervals. Data collected by the Sea-Bird CTD were processed using the Sea-Bird Scientific data processing software, Seasoft. Data collected by RBR CTDs were processed using the steps outlined in Halverson et al. (2017). All CTD data are available for download on the Hakai Data Portal (hecate.hakai.org) and at www.cioospacific.ca. Surface depths of CTD profiles varied due to the CTD system utilized and prevailing weather conditions. In general, profiles from the larger Sea-Bird CTD system began at 2–3 m depths, while casts with the smaller RBR systems generally started shallower (1 m). To maintain consistency across the time series, all CTD data shallower than 3 m depth were removed from analysis.

Similar to Masson and Peña (2009), water column stratification was characterized from CTD profiles using the difference between densities at 30 m and 3 m depths ($\Delta\rho$, kg m^{-3}). The 30 m depth threshold, used to define the base of the surface layer, was chosen to be consistent with Masson and Peña (2009) who found that most of the chlorophyll

variability occurred above this depth at stations across the Salish Sea. Furthermore, a Discovery Island regional study suggests that the majority of temperature and salinity variability also occurs above 30 m depth (Chandler et al. 2017). Water column stratification was further investigated using the Brunt-Väisälä (buoyancy) frequency averaged over 3–30 m depths; however, $\Delta\rho$ and this measure were highly correlated ($r^2 = 0.99$), providing confidence that $\Delta\rho$ was an accurate measure of upper water column stratification. As such, only $\Delta\rho$ is reported.

Freshwater inputs are an important component of stratification and stability in the NSoG (Masson and Peña 2009; Chandler et al. 2017; Evans et al. 2019) and were also investigated in this study. The freshwater content (FWC) of the upper water column was calculated using the method of Proshutinsky et al. (2009) following:

$$\text{FWC} = \frac{\int_{z_2}^{z_1} [S_{\text{ref}} - S(z)] dz}{S_{\text{ref}}}$$

where z represents water depth and S_{ref} is a reference salinity of 29.1. This reference salinity was selected to be in line with Evans et al. (2019) who used this calculation to characterize freshwater at station QU39. In this study, z_1 represents the shallowest bin (3 m) and z_2 represents the depth at the reference salinity. As such, variability in FWC represents the amount of freshwater accumulated above the 29.1 isohaline.

Water Samples

Nutrients

Macronutrients (nitrate + nitrite ($\text{NO}_3^- + \text{NO}_2^-$), phosphate (PO_4^{3-}), and silica (SiO_2)) were collected at 5 m depth, frozen at -20°C , and subsequently analyzed using a Lachat QuikChem 8500 Series 2 Flow Injection Analysis System at the University of British Columbia. Concentrations are reported as $\mu\text{mol L}^{-1}$. Limits of detection for $\text{NO}_3^- + \text{NO}_2^-$, PO_4^{3-} , and SiO_2 were $0.036 \mu\text{mol L}^{-1}$, $0.032 \mu\text{mol L}^{-1}$, and $0.1 \mu\text{mol L}^{-1}$, respectively (Mahara et al. 2019). Over the time series, 176 nutrient samples were used for analysis.

Phytoplankton Microscopy

From 2016 to 2018, microscopic analysis of phytoplankton species was performed on samples from 1 m depth (109 samples). Upon collection, samples were transferred into 250-mL amber glass bottles and immediately fixed using Lugol's solution (1% concentration). Sample bottles were kept cool and stored within a dark fridge until analysis was performed. Analysis was performed at LCJL Marine Ecological Services, and phytoplankton were enumerated using

Utermöhl settling chambers (50 mL) and phase-contrast microscopy utilizing an inverted light microscope (Utermöhl 1958). Phytoplankton cell count data were reported in cells L⁻¹.

Rather than direct analysis, microscopy data were used to help guide and support the interpretation of the Chemtax analysis. Direct analysis was not performed on the microscopy data due to lower data availability when compared to HPLC (i.e., no microscopy data was available in 2015) and the desire to study the whole phytoplankton community including small sized organisms not easily quantified via microscopy. Differences in sampling depths between the microscopy and pigment data may have also resulted in differences in species compositions between the two data types, especially during stable summer conditions.

HPLC and Chemtax Analysis

Phytoplankton biomass and composition were investigated using phytoplankton pigment concentrations derived from HPLC. Over the studied time series, 143 samples for HPLC analysis were collected at 5 m depth from Niskin bottles. For each sample, 1 L of water was vacuum filtered through a 47-mm glass fiber filter which was folded inwards, blotted to remove excess water, placed in folded aluminum foil, and then stored at -80 °C until analyzed. HPLC analyses were performed at the University of South Carolina Baruch Institute using the USC method (Hooker et al. 2005). Pigments derived from HPLC were then analyzed using Chemtax (v1.95), which applies matrix factorization to derive estimates of the biomass contribution of the main phytoplankton groups in terms of total chlorophyll *a* (mg TChla m⁻³) (Mackey et al. 1996). Pigments used for analysis, abbreviations, and associations with phytoplankton groups are shown in Table 1.

As complex phytoplankton assemblages have been observed in the region, the selection of Chemtax groups and pigment ratios was considered carefully and guided by the microscopic and pigment data. Following the grouping of Higgins et al. (2011), seven taxonomic groups were included in the Chemtax analysis: cyanobacteria 2 (Cyan), haptophytes 6–8 (Hapo), prasinophyte 3 (Pras), cryptophytes (Cryp), dinoflagellate 1 (Dino), dictyochophytes (Dict), and diatoms 1–2 (Diat). The selection of groups was based on the following:

- (a) Cyanobacteria 2 was selected as it is representative of temperate species. Zeaxanthin, also present in green algae, was deemed appropriate as a marker pigment for cyanobacteria as it showed little comparability with prasinoxanthin (a marker for prasinophytes; $r^2 = 0.35$), and zeaxanthin-to-Chlb ratios were greater than those generally found in prasinophytes ($\mu = 0.44 \pm 0.47$) (Schlüter and Møhlenberg 2003).

- (b) Pigment ratios for the haptophyte groups 6–8 were averaged as species from these groups were either observed or periodically bloom in the Salish Sea (i.e., *Emiliania huxleyi*, *Chrysotrichomonas* sp., and *Phaeocystis* sp., from Haigh et al. 1992; Peña and Nemcek 2017), but were difficult to separate via chemotaxonomy. Similar merging of groups has been performed elsewhere in the literature (Nunes et al. 2018).
- (c) Prasinophyte 3, representing prasinoxanthin-containing prasinophytes, was selected as prasinoxanthin showed higher concentrations than lutein (0.00–0.17 mg m⁻³ versus 0.00–0.02 mg m⁻³, respectively), was highly correlated with Chlb ($r^2 = 0.81$, $p < 0.001$), and showed a mean ratio with TChla (0.21) indicative of the group and suggestive of their overarching dominance (Schlüter and Møhlenberg 2003; Mendes et al. 2011; Nunes et al. 2018). Chlorophytes were not included in the analysis as their marker pigment, lutein, was almost always below detection levels, suggesting a lack of presence (Nunes et al. 2018). At times, other green algae (i.e., euglenophytes) may have played minor roles but were not separable via chemotaxonomy and, when present, would have been included in the prasinophyte 3 group.
- (d) Pigment ratios for cryptophytes were derived from measured pigment concentrations as there were multiple events when microscopy showed high abundances and dominance of cryptophyte species (largely *Hillea* sp.), but observed pigment ratios were considerably lower than those provided in the literature derived from species not observed locally. Ratios were computed by averaging Chlc₁₊₂:Tchl and Allo:TChla values when microscopy showed >90% relative cryptophyte abundance (Online Resource 1) spanning a range of environmental and biomass conditions.
- (e) Dinoflagellate 1 was selected as photosynthetic peridinin-containing dinoflagellates were dominant through the time series (*Gymnodinium* spp., *Gyrodinium* spp., and *Scrippsiella*).
- (f) For dictyochophytes, literature-derived pigment ratios were used with exception to 19BF, where instead of literature values, ratios from two events where dictyochophytes were observed in high abundance (*Dictyocha speculum/fibula* and *Apedinella spinifera*, Online Resource 2) were used since both events showed comparable 19BF ratios. It should be noted that pelagophytes and chrysophytes can show similar pigment profiles to dictyochophytes (separated via 19BF) so these groups are difficult to separate via Chemtax (Daubjerg and Henriksen 2001; Coupel et al. 2015; Vaillancourt et al. 2018) and may have been included in the dictyochophyte group. Chrysophytes were observed in the microscopy, but in relatively low abundance, and were never dominant. Pelagophytes were not

Table 1 HPLC marker pigments, their abbreviations used in the text, and the dominant phytoplankton groups that they are associated with based on the grouping of Higgins et al. (2011)

Pigment	Abbreviation	Groups
Total chlorophyll <i>a</i>	TChla	All photosynthetic groups
Chlorophyll <i>c</i> ₁₊₂	Chlc ₁₊₂	Diatoms, dictyochophytes, dinoflagellates, cryptophytes, haptophytes, pelagophytes, raphidophytes
Chlorophyll <i>b</i>	Chlb	Chlorophytes, prasinophytes, euglenophytes
Peridinin	Peri	Dinoflagellate 1
19'-Butanoyloxyfucoxanthin	19BF	Dominant in dictyochophytes and pelagophytes; present in dinoflagellate 2 and haptophytes 6–8
Fucoxanthin	Fuco	Dominant in diatoms; present in dictyochophytes, haptophytes, dinoflagellates, and synurophytes
19'-Hexanoyloxyfucoxanthin	19HF	Dominant in haptophytes 6–8; present in pelagophytes and dinoflagellate 2
Prasinoxanthin	Pras	Prasinophyte 3
Alloxanthin	Allo	Cryptophytes
Zeaxanthin	Zea	Dominant in cyanobacteria; present in some diatom 1, dinoflagellate 2, euglenophytes, prasinophytes, and raphidophytes
Lutein	Lut	Dominant in chlorophytes; present in prasinophytes and euglenophytes

observed and are not well described in the Salish Sea, but as they are pico-sized, they may have been missed by microscopic analysis. As such, it is possible that at times, pelagophytes contributed to the dictyochophyte group.

- (g) As species from both the diatom 1 and diatom 2 (largely *Pseudo-nitzschia*) groups were observed in the microscopy, literature ratios were averaged for use in Chemtax.

Selected pigment ratios for Chemtax analysis are shown in Table 2. Ratios were derived from the values in Higgins et al. (2011), except where specified. Following Wright et al. (2009), the selected ratios were randomized to create starting points for 60 Chemtax runs. This randomization step was performed on the input matrix for each additional Chemtax run described below.

Similar to Armbrecht et al. (2015), Chemtax was initially run on the entire time series (2015–2018) to optimize the literature-derived ratio matrix to the NSoG region. To minimize the effect of environmental variability on the pigment ratios (i.e., light and nutrient conditions), output ratios of the initial run were then input into further runs on seasonally binned data following the seasonal definitions in the section “Seasonal-Scale Analysis.” A single Chemtax run, using the output ratio matrix from the initial “seeding” run, was performed on each of the seasonal bins, and the output ratio matrices for each are provided in Online Resources 3–6.

Three bloom events (see Table 3) were missed by HPLC sampling and Chemtax analysis but were captured by 5 m depth fluorometrically derived chlorophyll (Chl, mg m⁻³) samples (47-mm GF filter, acidification method of Holm-Hansen et al. (1965)) and other parameters (fluorometrically derived size-fractionated Chl (> 20 µm), nutrients, microscopy). Due to the importance of these bloom events to seasonal biomass, it was necessary to incorporate them into the Chemtax time series to provide a representative dataset.

Dates and ancillary data suggest that each bloom was largely dominated by diatoms (Table 3). Considering this, a Chemtax estimate was created as follows: first, an HPLC TChla concentration for each point was derived from the linear relationship between corresponding fluorometric Chl and HPLC-derived TChla samples over the entire time series (TChla = 0.59Chl + 0.33, $r^2 = 0.81$). Secondly, based on the available evidence, the relative group contribution for each point was set to 100% diatoms. While diatoms dominated these bloom events, their contribution was likely not 100% of the total phytoplankton pool; however, it was impossible to estimate the small contributions from other groups. As such, compositions from these estimated points should be considered with care and are clearly marked when used.

Diversity Index

Phytoplankton community diversity was investigated using the Shannon-Weaver Index:

$$H = \sum_{i=1}^N P_i \ln[P_i]$$

In this equation, P_i is the proportion of each Chemtax-derived phytoplankton group biomass relative to TChla biomass (%) and N is the number of input groups. This application of the Shannon Diversity Index has been used by other authors to effectively characterize phytoplankton group diversity (Lohrenz et al. 2003; Latasa et al. 2010).

Seasonal-Scale Analysis

To investigate interannual seasonal-scale variability, phytoplankton and physical data were averaged into seasonal bins. Seasonal bins followed traditional meteorological definitions:

Table 2 Pigment:TChla ratios input into the initial seeding Chemtax run

Group	Chl c_{1+2}	Peri	19BF	Fuco	19HF	Pras	Allo	Zea	Lut	Chlb	TChla
Cyan	0	0	0	0	0	0	0	0.64	0	0	1
Hapt	0.21	0	0.04	0.31	0.47	0	0	0	0	0	1
Pras	0	0	0	0	0	0.25	0	0.06	0.01	0.70	1
Cryp	0.05	0	0	0	0	0	0.07	0	0	0	1
Dino	0.22	0.56	0	0	0	0	0	0	0	0	1
Dict	0.11	0	0.10	0.35	0	0	0	0	0	0	1
Diat	0.23	0	0	0.89	0	0	0	0	0	0	1

Winter (December 21–March 20), Spring (March 21–June 20), Summer (June 21–September 20), and Autumn (September 21–December 20). As the time series began in 2015, the 2015 winter season lacks data from December 2014; however, no data points exist over the brief December winter period in any of the following years. Therefore, the seasonal averaging should be consistent across the time series.

Multivariate Statistical Analysis

We performed redundancy analysis (RDA), a constrained ordination technique, to investigate the effect of environmental drivers on Chemtax phytoplankton group biomass. Redundancy analysis is a commonly used ecological method suited to exploring relationships between environmental data and species abundance across a range of environmental gradients and has been previously utilized in Chemtax-based phytoplankton studies (Ramette 2007; Vaillancourt et al. 2018). All of the following transformations, checks and statistical analysis were performed in R using the vegan statistical package (Oksanen et al. 2019; R Core Team 2019).

Redundancy analysis was performed on 138 samples with matching response (7 Chemtax phytoplankton groups) and explanatory (temperature, salinity, $\Delta\rho$, FWC, $\text{NO}_3^- + \text{NO}_2^-$, PO_4^{3-} , SiO_2 , wind speed, and solar radiation) variables. Prior to analysis, response variables (Chemtax groups) were transformed using the Hellinger transformation to increase suitability for the linear-based RDA and giving groups with low- or zero-biomass reduced weights (Legendre and Gallagher 2001; Ramette 2007). To ensure applicability of the linear RDA, a detrended correspondence analysis (DCA) was performed on the explanatory variables and the result showed a gradient value of < 3 SD

(1.87), indicating that the RDA method was the appropriate selection for the data (Ramette 2007). After the above transformations and checks were complete, a global RDA model was performed using all explanatory variables to check for global significance, which allows for continuation with a forward selection model (global model was significant to $p < 0.001$ using permutation tests (999)) (Blanchet et al. 2008). Following the global check, a forward-stepwise RDA was performed (using the OrdinR2step function which corrects for the overestimation of explained variance) to remove explanatory variables that did not significantly ($p > 0.05$) contribute to variation in the response data with significance determined via Monte Carlo permutations (49,999) (Ramette 2007; Blanchet et al. 2008; Vaillancourt et al. 2018). As a result, salinity, FWC, PO_4^{3-} , wind speed, and solar radiation were removed from the RDA since they were not found to be significant explanatory variables.

Results

Environmental Influences on Phytoplankton Biomass

The 2015–2018 time series of phytoplankton biomass (mg TChla m^{-3}) plotted against wind speed (m s^{-1}), solar radiation (W m^{-2}), $\Delta\rho$ (kg m^{-3}), $\text{NO}_3^- + \text{NO}_2^-$ ($\mu\text{mol L}^{-1}$), and SiO_2 ($\mu\text{mol L}^{-1}$) is shown in Fig. 2 (plots of temperature, salinity, and PO_4^{3-} are provided in Online Resource 7). Each year showed a distinct spring bloom (defined as the first day of the year when $\text{TChla} > 5 \text{ mg m}^{-3}$, following Gower et al. (2013)) associated with sharp decreases in $\text{NO}_3^- + \text{NO}_2^-$ and SiO_2 (Fig. 2d, e). Spring bloom timing and biomass varied widely among years with initiation dates and TChla

Table 3 Available ancillary data for estimated TChla concentrations where Chemtax group compositions were set to 100% diatoms

Date	% Chl > 20 μm (%)	Chl (mg m^{-3})	TChla estimated (mg m^{-3})	Dominant species
2015-02-24	96	20.46	12.40	NA
2016-04-01	95	18.98	11.53	<i>Chaetoceros</i> sp.
2016-08-22	88	8.88	5.57	<i>Chaetoceros socialis</i>

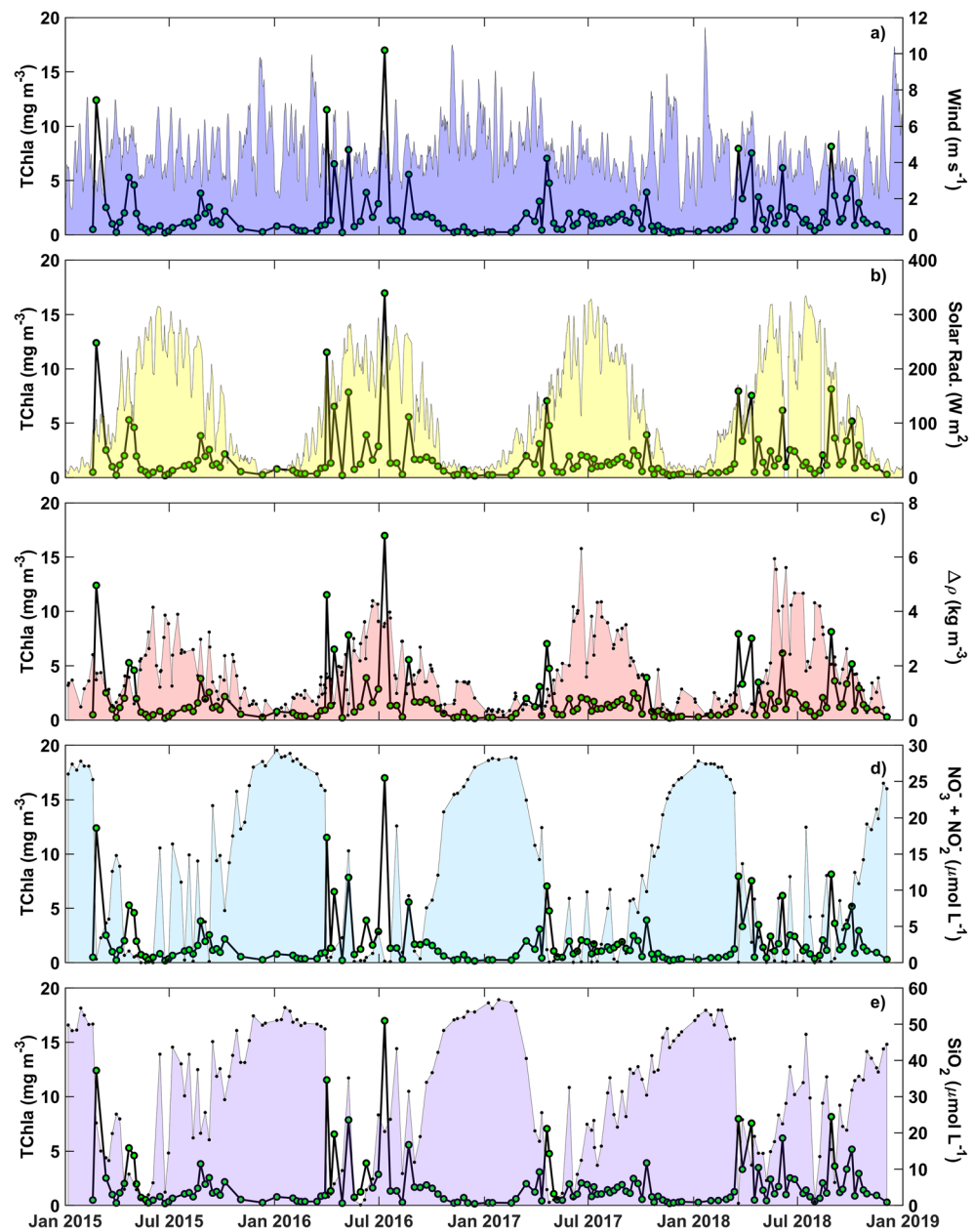
concentrations being February 24, 2015 ($12.40 \text{ mg TChla m}^{-3}$); April 1, 2016 ($11.53 \text{ mg TChla m}^{-3}$); April 20, 2017 ($7.05 \text{ mg TChla m}^{-3}$); and March 20, 2018 ($7.95 \text{ mg TChla m}^{-3}$). In each year, the spring bloom contributed 22.5%, 14.7%, 12.3%, and 9.5% of total annual phytoplankton biomass, respectively. The 2015 and 2016 spring bloom dates match those found by Mahara et al. (2019) at station QU39.

While no statistically significant trends between phytoplankton and solar radiation or winds were observed, most of the spring blooms developed following sunny and calm periods. For instance, the early and high biomass 2015 spring bloom was associated with an early period of increased solar radiation, less windy conditions, and increased stratification. Backward running daily mean incoming solar radiation spiked

on February 18 to 86.8 W m^{-2} and persisted, peaking on February 24 at 107.8 W m^{-2} . Backward running daily mean winds remained $< 5 \text{ m s}^{-1}$, from February 12 through to mid-March.

The 2016 bloom, which occurred 5 weeks later than 2015, also occurred during a spike in solar radiation (backward running daily mean incoming solar radiation peaked on April 1, 2016 = 217.9 W m^{-2}) and a brief abatement of winds (backward running daily mean wind on April 1, 2016 = 3.2 m s^{-1}) with backward running daily mean winds being below or close to 5 m s^{-1} from March 17, 2016 through to April 12, 2016. Increased stratification also coincided with these calm conditions. While light levels reached those of 2015 earlier than the observed bloom initiation, these events were

Fig. 2 Northern Strait of Georgia (NSoG) time series of station QU39 5 m depth HPLC-derived TChla (mg m^{-3} , green dots) associated with the left y-axis of each panel and on the right y-axis where it is plotted against (a) Environment Canada Sentry Shoal buoy (46131) wind speed (m s^{-1}), (b) Hakai Institute field station incoming solar radiation (W m^{-2}), (c) QU39 $\Delta\rho$ (kg m^{-3}), (d) QU39 5 m depth $\text{NO}_3^- + \text{NO}_2^-$ ($\mu\text{mol L}^{-1}$), and (e) QU39 5 m depth SiO_2 ($\mu\text{mol L}^{-1}$). Both solar radiation and wind speed were smoothed using 4-day backward moving daily averages (3 days prior and day of)



generally of short duration. Furthermore, the bloom was preceded by a long-term wind event which spanned much of March. The latest bloom in 2017 was preceded by long-term persistent winds and was initiated directly following their abatement. In 2018, the bloom was initiated at the end of a clearly defined period of increased solar radiation and low wind (generally $> 100.0 \text{ W m}^{-2}$ and $< 5.0 \text{ m s}^{-1}$ from March 5 to 24).

Following the spring bloom and its associated nutrient drawdown in each year, several peaks in upper layer $\text{NO}_3^- + \text{NO}_2^-$ and SiO_2 concentrations were observed through the spring and summer seasons which appear to be associated with wind events. Many, but not all, of these nutrient peaks were associated with sporadic increases in phytoplankton biomass. The majority of post-spring blooms occurred in 2016 (4) and 2018 (4), with the largest biomass event occurring on July 11, 2016 ($16.99 \text{ mg TChla m}^{-3}$). This event was unique in that it was associated with an increase in surface $\text{NO}_3^- + \text{NO}_2^-$ and high SiO_2 , under relatively stratified surface layer conditions with $\Delta\rho$ being $> 3.00 \text{ kg m}^{-3}$ from June 9 through July 29, 2016, compared to periodic dips below $< 2.50 \text{ kg m}^{-3}$ in other years. In each year, several short-lived summer increases in surface $\text{NO}_3^- + \text{NO}_2^-$ were observed but were not associated with increased phytoplankton biomass. In particular, 2017 showed no post-spring blooms despite three $\text{NO}_3^- + \text{NO}_2^-$ spikes between spring and the end of summer.

Late summer/early autumn increases in phytoplankton biomass were observed every year and were usually associated with nutrient reintroduction to the surface layer. However, 2018 was the only year to show a true and long-lasting autumn bloom ($> 5.00 \text{ mg TChla m}^{-3}$, post September 21) that was observed under high nutrient conditions and directly following late season increases in solar radiation. For instance, the bloom peak on October 4, 2018, occurred following a peak in backward running daily mean solar radiation on September 29 (151.10 W m^{-2}); however, similar or greater peaks in solar radiation were observed in years when autumn blooms did not occur.

Phytoplankton biomass was low ($< 1.00 \text{ mg TChla m}^{-3}$) from late autumn (i.e., November) through late winter (i.e., February) in all years.

Trends in Phytoplankton Compositions

Links with Environmental Drivers

Results of the RDA suggest diatoms were negatively correlated to all groups except dinoflagellates (arrows pointing in opposite directions) and were largely associated with the spring and autumn seasons (Fig. 3). In turn, the haptophyte, dictyochophyte, and cyanobacteria groups were positively correlated (arrows pointing in similar directions) and

associated with the summer season. Prasinophytes and cryptophytes were positively correlated and formed their own ordination grouping that did not appear to be linked to a specific season.

The amount of variance in the phytoplankton groups explained by the explanatory (environmental) variables was as follows: temperature (21%, $p < 0.001$), SiO_2 (11%, $p < 0.001$), $\text{NO}_3^- + \text{NO}_2^-$ (2%, $p < 0.050$), and $\Delta\rho$ (2%, $p < 0.050$). Negative correlations existed between diatoms, temperature, and $\Delta\rho$. In contrast to diatoms, the ordination plot suggests that cyanobacteria, haptophytes, and dictyochophytes all showed strong positive correlations with both temperature and $\Delta\rho$. Prasinophytes and cryptophytes were not as strongly related to temperature or $\Delta\rho$ (arrows nearly orthogonal) but did show weak positive correlations with macronutrients suggesting presence during high nutrient periods. Dinoflagellates were unique showing positive correlations with both SiO_2 and $\text{NO}_3^- + \text{NO}_2^-$.

Blooming Conditions

Spring blooms were dominated by large fast-growing diatoms that resulted in low group diversity, as indicated by the lower Shannon Diversity Index during these bloom events (Fig. 4 and Fig. 5). The spring blooms were primarily composed of *Skeletonema* or *Chaetoceros* sp. (Table 4), except for the 2018 spring bloom that included small-sized non-colonial *Phaeocystis pouchetii* (Hapt); however, Chemtax analysis showed a very minor biomass contribution ($0.20 \text{ mg TChla m}^{-3}$, 0.3%) by this group.

Blooms that occurred after the spring bloom were largely comprised of diatoms, with late spring and summer blooms primarily composed of *Chaetoceros* sp. The 2018 late summer and autumn blooms showed high numbers of *Pseudonitzschia seriata* (Table 4), which was the only occasion this species was abundant. The only observed non-diatom dominated bloom occurred on July 11, 2016, and was dominated by *Dictyocha* species and also included small-celled *Skeletonema marinoi* and large-sized *Eucampia zodiacus*. Chemtax-derived dictyochophyte and diatom biomass for this bloom were $8.23 \text{ mg TChla m}^{-3}$ (49%) and $7.29 \text{ mg TChla m}^{-3}$ (43%), respectively. This bloom formed the timeseries maximum biomass and followed an increase in surface $\text{NO}_3^- + \text{NO}_2^-$ and surface stratification. Additionally, the bloom coincided with increased surface freshwater content (2.2 m) and temperature (16.7°C) (Fig. 6).

Non-blooming Conditions

Under non-blooming conditions, diverse phytoplankton communities emerged, and as a result, Shannon Index values increased (1.0–2.0, Fig. 5). Diatom contributions declined but remained important through the year, typically contributing

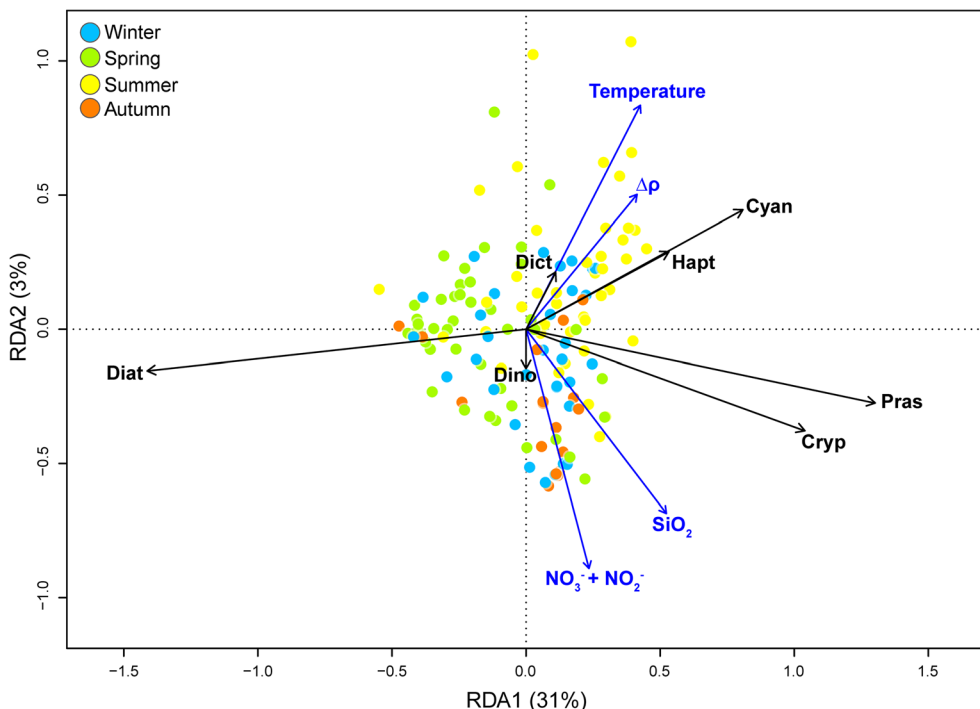


Fig. 3 RDA triplot (scaling 2) for the 2015–2018 QU39 time series. Chemtax data were transformed using a Hellinger transformation. Blue arrows represent the statistically significant explanatory variables (temperature, $\Delta\rho$, $\text{NO}_3^- + \text{NO}_2^-$, and SiO_2), and black arrows represent the seven Chemtax phytoplankton groups. Sampling points are shown as points color coded by season as defined in the section “Seasonal-Scale Analysis.” The global model was significant ($p < 0.001$) with the

environmental variables explaining 36% of the constrained variance in the Chemtax phytoplankton groups. RDA axis 1 was significant to $p < 0.001$ and RDA axis 2 to $p < 0.010$. In this plot, the angle between any two arrow vectors represents the linear correlation between the two variables. Arrows at 90° to each other show no correlation to one another ($r = 0$), arrows $< 90^\circ$ to each other have a positive correlation ($0^\circ, r = 1$), and those $> 90^\circ$ have negative correlations ($180^\circ, r = -1$)

20 to 40% of TChla biomass. Outside of diatoms, dominant groups with persistent contributions were prasinophytes (0–0.86 mg TChla m^{-3} , 0–44%) and cryptophytes (0–0.99 mg TChla m^{-3} and 0–47%), both of which were important during non-blooming periods throughout the year and whose biomass contributions generally peaked between late spring and summer. In turn, cyanobacteria showed important contributions (0–0.64 mg TChla m^{-3} and 0–58%) but were only present and showed peak biomass during the summer and autumn seasons.

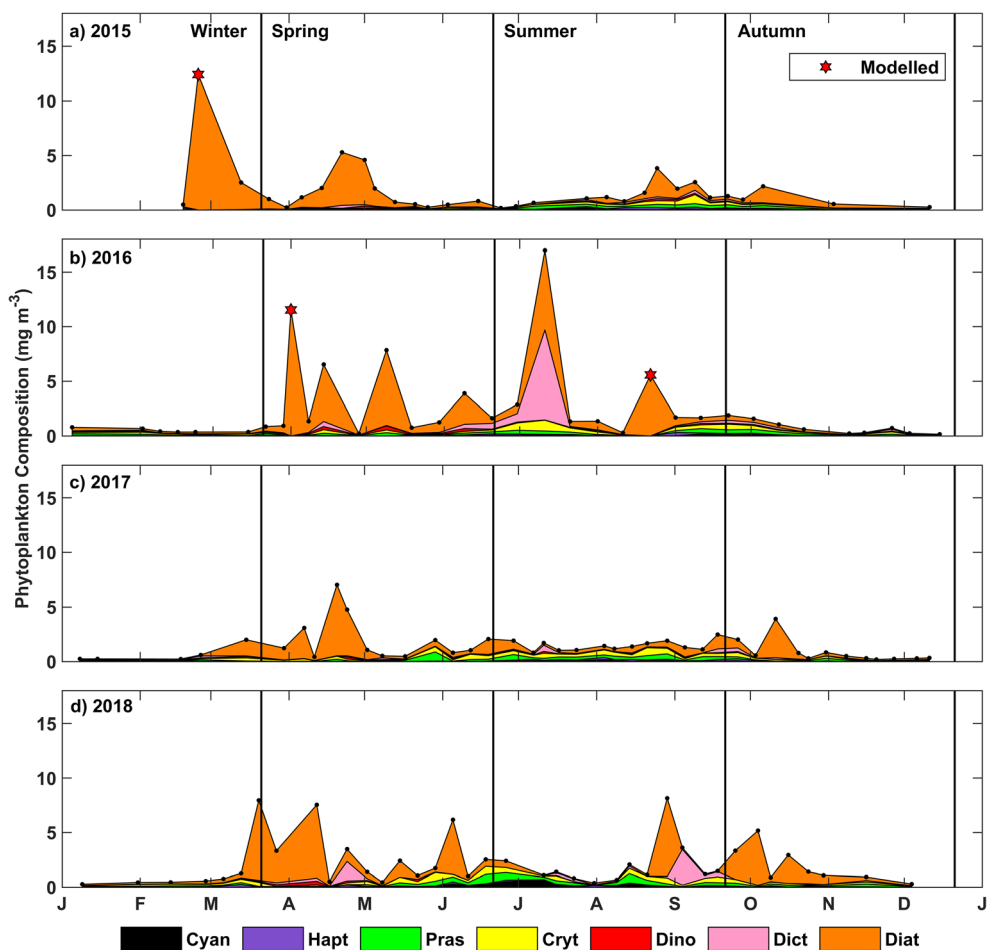
The 2018 late spring and summer seasons were unique in that they showed some of the highest and most persistent biomass contributions by prasinophytes, cryptophytes, and cyanobacteria (Fig. 6b). Over the period between June and September 2018, three events with reductions in stratification, temperature, and nutrient renewal ($\text{NO}_3^- + \text{NO}_2^- > 10 \mu\text{mol L}^{-1}$) were observed (Fig. 6d, f). Following each event, $\text{NO}_3^- + \text{NO}_2^-$ was drawn down ($< 0.2 \mu\text{mol L}^{-1}$) and prasinophyte and cryptophyte biomass increased rather than diatom biomass. Between nutrient renewal events, the time series maximum cyanobacterial biomass (July 11, 0.64 mg TChla m^{-3} , 58%) occurred under highly stratified ($\Delta\rho = 4.67 \text{ kg m}^{-3}$), warm (15.51°C), and nutrient-depleted ($\text{NO}_3^- + \text{NO}_2^- = 0.17 \mu\text{mol L}^{-1}$) conditions.

Through the time series, neither haptophytes (0–0.30 mg TChla m^{-3} and 0–40%) nor dinoflagellates (0–0.37 mg TChla m^{-3} and 0–19%) showed large biomass contributions to the phytoplankton community. There was a single event, on September 4, 2018, where haptophytes (*Phaeocystis pouchetii*) were observed in high abundance microscopically but were misclassified by Chemtax as dictyochophytes (3.27 mg TChl m^{-3} , 90%) (Fig. 4, Table 4). During this event, the concentration of the haptophyte marker pigment 19HF was below levels of detection and the marker typically associated with dictyochophytes, 19BF, had a relatively high concentration (0.74 mg TChla m^{-3}). Photosynthetic dinoflagellates were never a dominant group either within the Chemtax-derived phytoplankton biomass or microscopy data. Microscopy showed that cell counts never exceeded 9000 cells L^{-1} for any identifiable photosynthetic dinoflagellate species.

Seasonal-Scale Comparisons of Phytoplankton Composition and Physical-Chemical Drivers

Seasonal average Chemtax-derived phytoplankton composition and selected environmental variables are presented in Fig. 7. In general, they show a seasonal cycle with

Fig. 4 Station QU39 time series of weekly to bi-weekly phytoplankton groups (in mg TChla m⁻³) at 5 m depth derived from Chemtax in (a) 2015, (b) 2016, (c) 2017, and (d) 2018. Vertical black lines indicate seasonal delineations used in the seasonal-scale analysis (see section “Seasonal-Scale Analysis”). Points marked with red stars are estimated concentrations (section “HPLC and Chemtax Analysis”) used when Chemtax data were unavailable



biomass increasing from winter (1.59 mg TChla m⁻³) to spring (2.39 mg TChla m⁻³) and then declining from summer (2.06 mg TChla m⁻³) through autumn (1.13 mg TChla m⁻³) (Fig. 7a). Compositonally, biomass was dominated by diatoms in winter (80%) and spring (76%) followed by

a more diverse community in summer and autumn made up of dictyochophytes (19% and 6%, respectively), prasinophytes (13% and 12%, respectively), cryptophytes (16% and 13%, respectively), and cyanobacteria (5% and 4%, respectively).

Fig. 5 Station QU39 2015–2018 5 m depth time series of weekly to biweekly (a) Phytoplankton relative composition (%) derived from Chemtax. (b) Shannon Diversity Index (shaded purple area, left y-axis) and TChla (black line with green dots, right y-axis). Higher diversity index values represent increased phytoplankton group diversity while lower values represent a more homogenous composition. Points marked with red stars and where diversity index values decline to zero are estimated concentrations (section “HPLC and Chemtax Analysis”) used when Chemtax data were unavailable

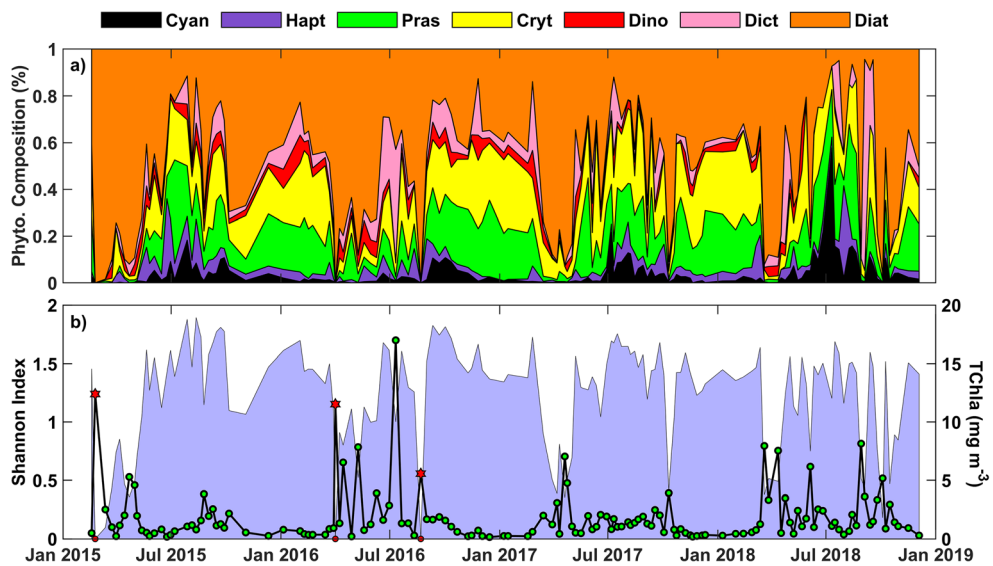


Table 4 Dates, associated season, dominant species from microscopic identification, and microscopy cell counts (cells L^{-1}) for bloom events where data were available

Date	Season	Species (group)	Cells (L^{-1})
2016-04-14	Spring	<i>Chaetoceros cinctus</i> (Diat)	448,000
2016-05-09	Spring	<i>Skeletonema marinoi</i> (small) (Diat)	2,856,000
2016-07-11	Summer	<i>Dictyocha</i> spore (Dict)	146,200
		<i>Dictyocha fibula</i> (Dict)	37,800
2016-08-22	Summer	<i>Chaetoceros socialis</i> (Diat)	3,376,538
		<i>Chaetoceros danicus</i> (Diat)	2,778,038
2017-04-20	Spring	<i>Skeletonema marinoi</i> (Diat)	110,600
		<i>Chaetoceros socialis</i> (Diat)	92,600
		<i>Chaetoceros debilis</i> (Diat)	69,600
2017-04-24	Spring	<i>Chaetoceros socialis</i> (Diat)	243,648
2018-03-20	Spring	<i>Skeletonema marinoi</i> (Diat)	486,356
		<i>Chaetoceros debilis</i> (Diat)	324,768
		<i>Thalassiosira rotula</i> (Diat)	127,360
		<i>Phaeocystis pouchetii</i> (Hapt)	928,025
2018-04-12	Spring	<i>Chaetoceros socialis</i> (Diat)	745,500
2018-05-06	Summer	<i>Eucampia zodiacus</i> (Diat)	38,554
2018-08-29	Summer	<i>Pseudo-nitzschia seriata</i> (Diat)	310,000
2018-09-04	Summer	<i>Pseudo-nitzschia seriata</i> (Diat)	303,030
		<i>Phaeocystis pouchetii</i> (Hapt)	322,787
2018-08-29	Autumn	<i>Pseudo-nitzschia seriata</i> (Diat)	555,720
2018-10-04	Autumn	<i>Pseudo-nitzschia seriata</i> (Diat)	196,000

As shown by the interannual seasonal variability (Fig. 7b–e), the time series mean winter biomass and composition were largely skewed by the early and strong 2015 spring bloom, which occurred well before the transition to spring season (February 24). Among years, the 2015 winter season showed the highest mean biomass ($5.14 \text{ mg TChla m}^{-3}$) dominated by diatoms (98%). In comparison, the 2016 winter season showed considerably lower biomass ($0.50 \text{ mg TChla m}^{-3}$) and a diverse suite of phytoplankton groups (Diat = 36%, Cryp = 25%, and Pras = 20%) more representative of true winter conditions. Hence, interannual variability of seasonal mean biomass is highly influenced by the timing and occurrence of episodic bloom events, as also seen in the 2016 summer mean, which was largely driven by the silicoflagellate (*Dictyocha* sp.) bloom (Fig. 7d), and the 2018 summer and autumn seasonal means that were driven by diatom (*Pseudo-nitzschia*) blooms (Fig. 7e). In summary, relatively short-lived high biomass blooms drove seasonal and interannual biomass variability at station QU39.

In comparison to the groups that displayed blooms, interannual seasonal variability of prasinophytes, cryptophytes, and cyanobacteria was less pronounced, but some key differences were apparent. For example, the 2018 spring season showed greater contributions by prasinophytes (0.23 mg

TChla m^{-3} , 9%) and cryptophytes ($0.29 \text{ mg TChla m}^{-3}$, 11%) than those in previous years due to an earlier succession from the spring diatom bloom to a more diverse summer community (Fig. 7c). For the summer season, both 2017 and 2018 showed greater prasinophyte biomass when compared to prior years (Fig. 7d). The 2018 summer season showed the highest annual mean biomass by both prasinophytes and cyanobacteria ($0.32 \text{ mg TChla m}^{-3}$ and $0.20 \text{ mg TChla m}^{-3}$, respectively), and while the mean summer season prasinophyte biomass was only slightly higher than those of previous years ($0.21\text{--}0.28 \text{ mg TChla m}^{-3}$), mean cyanobacterial biomass was more than double than those observed in 2015–2017 ($0.06\text{--}0.09 \text{ mg TChla m}^{-3}$). The early spring-summer succession and increased summer flagellate and prokaryote biomass occurred without obvious seasonal-scale differences in the physical environment.

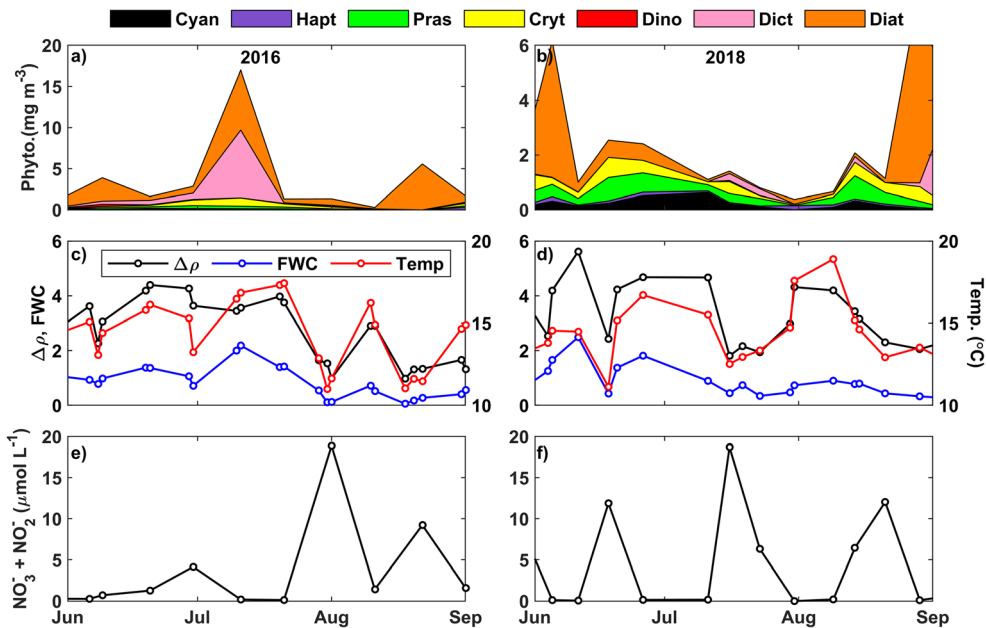
The physical and chemical data also showed a distinct seasonal cycle with 5 m depth temperature (Fig. 7f) and $\Delta\rho$ (Fig. 7q) increasing from winter to a summer maximum and then decreasing in autumn. FWC and SiO_2 showed different seasonal trends: While both were high in winter, FWC peaked in spring and then decreased to a minimum in autumn (Fig. 7l) and SiO_2 decreased to a minimum in spring and increased towards autumn (Fig. 7v). All of these parameters showed comparable annual seasonal means with a few exceptions: The warmest winters were observed in 2015 and 2016 (Fig. 7h), the most stratified winter was observed in 2015 (Fig. 7r), and the highest FWC was observed in the winter of 2015 (Fig. 7m).

Discussion

Seasonal Biomass

From 2015 to 2018, spring bloom timing varied widely, spanning the entire expected range from late February to mid-April (Collins et al. 2009; Allen and Wolfe 2013). This wide range was associated with varying oceanographic and atmospheric conditions. In the Strait of Georgia, spring blooms are initiated when there is adequate light available for surface phytoplankton, through a combination of decreased winter winds (that results in a shallower mixing layer) and decreased clouds (Collins et al. 2009; Masson and Peña 2009; Allen and Wolfe 2013). Variability of winter wind energy and cloud fractionation have been found to be the most prominent drivers of bloom timing (Collins et al. 2009; Allen and Wolfe 2013). In addition, warmer winter temperatures have also been associated with early blooms (Allen and Wolfe 2013; Suchy et al. 2019). Considering the above factors, the early 2015 bloom was likely a result of the low winds and sunny conditions observed prior to initiation, but also potentially warmer temperatures and increased stratification. In this

Fig. 6 Station QU39 2016 and 2018 June–September time series of (a and b) 5 m depth Chemtax-derived phytoplankton groups (in mg TChl m^{-3}); (c and d) $\Delta\rho$ ($kg\ m^{-3}$, black lines), FWC (blue lines), and 5 m depth temperature ($^{\circ}C$, red lines, right y-axis); and (e and f) 5 m depth $NO_3^- + NO_2^-$, ($\mu mol\ L^{-1}$). Note that the scales are different between (a) and (b)



year, the studied region was impacted by the 2014 to 2016 marine heatwave (Bond et al. 2015) that led to anomalously warm, stable winter weather over the British Columbia coast and increased winter runoff (Chandler 2016). In contrast, persistently strong winds likely delayed the 2017 spring bloom. Comparatively, the more typical timing of the 2016 and 2018 blooms did not show a strong and clear link with anomalous physical variables.

Spring bloom magnitudes were variable and it is possible that some of this variability can be explained by zooplankton grazing. At station QU39, there is evidence that increased spring zooplankton abundance occurs over a narrow temporal range in late March to early April, regardless of spring bloom timing (Mahara et al. 2019). The early 2015 spring bloom was the strongest of the time series and occurred outside of the expected peak zooplankton timing, and thus, grazing pressure may have exerted less of an influence when compared to the following years. Yet, the timing of the 2016 and 2018 spring blooms both occurred near the expected peak in zooplankton abundance and had large differences in observed biomass. The lower observed biomass in 2018 may be explained by the increase in wind stress directly following the spring bloom initiation, which could have increased losses due to mixing, surface layer dilution, and sinking. Following initiation, strong wind events have been shown to quickly reduce spring bloom biomass and create a lag before phytoplankton accumulation resumes and bloom conditions redevelop (Yin et al. 1996).

In the Strait of Georgia, bloom termination has been attributed to both nutrient limitation and increased grazing pressure (Harrison et al. 1983; Collins et al. 2009; Allen and Wolfe 2013; Peña et al. 2016). The results of this study suggest that at station QU39, bloom termination was driven by nutrient

limitation with nitrate concentrations falling below half saturation constants in each year. This finding is in contrast to the modeling results of Peña et al. (2016) who found that on average, zooplankton grazing was the primary driver of spring bloom termination in the Strait of Georgia; however, the discrepancy could be due to the difference in scales between studies (i.e., single station versus regional modeling) as regional phytoplankton dynamics are highly variable. In the Salish Sea, care must be taken to extend findings over broad geographic regions as spatial patchiness and variability are high and driven by a complex web of localized and broad-scale physical and environmental factors (Suchy et al. 2019).

Diatom-dominated post-spring blooms during the spring and summer seasons were a regular occurrence throughout the time series. In line with previous studies, these blooms appear to have been driven by wind or tidal events reintroducing nutrients to the surface layer and spurring new production (Collins et al. 2009; Peña et al. 2016). Regionally, vertical advection of nutrients has been found to be the primary source of nitrate into the surface layer, with nitrate being the dominant limiting nutrient (Harrison et al. 1983; Peña et al. 2016). This trend of vertical advection was partially confirmed via the RDA utilized in this study with diatom biomass being tied to both reductions in temperature and stratification suggesting mixing: Reductions in surface temperature have previously been linked to wind-driven mixing in the NSoG (Evans et al. 2019).

Yet, there were departures from this trend of increased biomass following surface nutrient injections and these are notable observations from this time series. First, the time series maximum biomass (*Dictyocha* sp.; July 11, 2016) occurred under warm, stratified, low-nutrient surface conditions

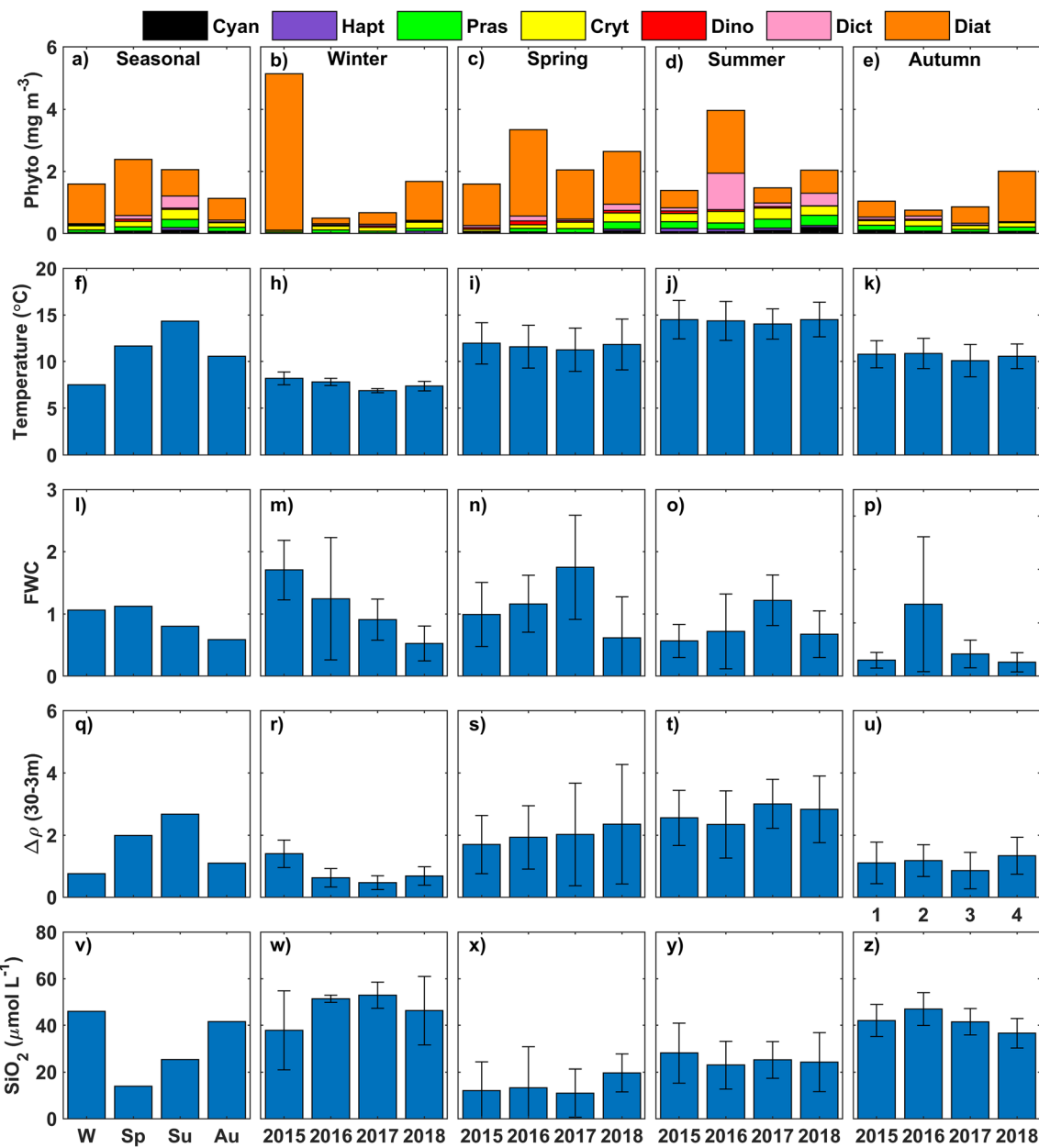


Fig. 7 Mean QU39 (a) time series wide seasonal trends and (b–e) mean annual winter, spring, summer, and autumn trends (separated by column) for 5 m depth TChla biomass (mg TChl m^{-3}) and Chemtax-derived phytoplankton composition; (f–k) CTD-derived 5 m depth temperature

($^{\circ}\text{C}$); (l–p) CTD-derived FWC; (q–u) CTD-derived $\Delta\rho$ (kg m^{-3}); and (v–z) 5 m depth SiO_2 ($\mu\text{mol L}^{-1}$). Seasonal-scale averaging was done following the section “Seasonal-Scale Analysis”

with high freshwater content (described further in the section “Bloom conditions”). Second, there were multiple events where nutrients were introduced into the surface layer and a corresponding diatom bloom was not observed. These nutrient introductions were followed by quick nutrient drawdown and as this is only achieved via phytoplankton uptake, increases in production, but not accumulation, must have occurred (Moore et al. 2013; Tiselius et al. 2016).

Processes that could account for low summer phytoplankton abundance despite nutrient renewal and drawdown include aggregation and sinking of cells and zooplankton

grazing. Although not specifically studied, past research has shown that in the Salish Sea, summer losses through aggregation and sinking of phytoplankton are relatively small compared to other loss processes (Peña et al. 2016). On the other hand, regional models have suggested that zooplankton grazing is an important regulator of summer diatom production (Peña et al. 2016). Similar events of increased nutrients, but a lack of net phytoplankton growth, have been observed in the Salish Sea and attributed to increases in copepod abundance (Yin et al. 1996). These results are comparable to other temperate oceans such as the Gullmar Fjord on the west coast of

Sweden where zooplankton grazing limits the accumulation of summer phytoplankton biomass through nutrient renewal events (Tiselius et al. 2016). Therefore, it is possible that strong top-down controls from grazing limited the post-spring and summer accumulation of diatoms, which are the primary bloom formers in the Strait of Georgia. Together, nutrient limitation and zooplankton grazing on diatoms could result in the observed extended periods of relatively low phytoplankton biomass and diverse phytoplankton community composition during summer. Future studies that focus on zooplankton grazing in the NSoG could shed light on the impact of zooplankton on phytoplankton biomass and composition.

Phytoplankton Compositions

Bloom Conditions

As in many temperate coastal regions, diatoms were the primary bloom-forming species and made dominant contributions to annual biomass in each year (Harrison et al. 1983; Seoane et al. 2006; Latasa et al. 2010; Goela et al. 2014; Nemcek et al. 2019). Under ideal high nutrient and light conditions, diatoms have the ability to quickly respond and accumulate biomass until resources become limiting or losses match or exceed new production (Carstensen et al. 2015). Based on previous research, the bloom-forming diatom species, largely *Skeletonema* spp., *Chaetoceros* spp., and *Pseudo-nitzschia*, were expected for this study area (Harrison et al. 1983). Similarly, the co-development of diatom blooms and *Phaeocystis* sp. observed in the spring of 2018 is common in coastal waters (Ansotegui et al. 2003; Simo-Matchim et al. 2017).

A novel event of the time series was the development of the large *Dictyocha* sp. bloom in July 2016. Blooms of this species, notably in the athenate (or naked/spore phase), have occasionally been observed in the region (Haigh et al. 1992). Both regionally and in other areas such as the Mediterranean Sea, drivers of *Dictyocha* sp. blooms remain elusive but have been linked to storm activity and increased runoff (Haigh et al. 1992; Rigual-Hernández et al. 2010). RDA failed to find a link between FWC (or salinity) and the dictyochophyte group; however, a notable increase in upper layer FWC was observed during the 2016 *Dictyocha* bloom. Furthermore, both stratification and temperature, which were linked to the dictyochophyte group through RDA, concurrently increased with FWC, suggesting that all of these factors may have played a role in bloom development. Interestingly, the observed temperature during the bloom (5 m–16.7 °C) was greater than the range expected for optimum growth (11.0–15.0 °C) of naked stage cells, which are sensitive to heat (Jochem and Babenerd 1989; Henriksen et al. 1993); however, it is possible that the water temperature was cooler when the bloom was initiated. As this bloom was observed

throughout the northern and central portions of the SoG (Esenkulova and Pearsall 2017; Pawlowicz et al. 2020), it is difficult to ascertain the source of the warm, fresh, and stratified surface waters that may have promoted its development. Late spring 2016 Fraser River discharge was anomalously high (Chandler 2017), and it is possible that this water extended northward creating the observed conditions; although, the many other freshwater sources to the NSoG (including large glacially fed rivers and smaller rivers) could have had a more direct influence on QU39 (Harrison et al. 1983; Foreman et al. 2015; Peña et al. 2016; Suchy et al. 2019). High rainfall observed before bloom onset may have further driven freshwater inputs from local sources (Esenkulova and Pearsall 2017).

The strong 2018 late summer and autumn *Pseudo-nitzschia* bloom was also unique to the time series, but it is common for late summer/autumn blooms to appear sporadically in the NSoG (Suchy et al. 2019). Similar to the overarching trends and those suggested by the RDA, this bloom appeared after an increase in surface nitrate driven by a mixing event, but it is interesting to note that two prior nutrient pulses did not incite earlier blooms possibly due to grazing pressure. Alternatively, similar to the *Dictyocha* sp. bloom, this bloom extended over a wide area of the NSoG (Esenkulova and Pearsall 2019; Nemcek et al. 2019). As such, it is also possible that both blooms were advected to the NSoG sampling location as surface water residence times in the region are expected to be at most a few days and wind-driven advection has been shown to have large-scale influences (Pawlowicz et al. 2007; Evans et al. 2019).

Non-bloom Conditions

The observed increase in phytoplankton community diversity under non-bloom conditions is common in temperate coastal systems (Harrison et al. 1983; Haigh et al. 1992; Ansotegui et al. 2003; Latasa et al. 2010; Goela et al. 2014; Carstensen et al. 2015). Of the observed groups, the prasinophyte and cryptophyte groups were the most persistent, being dominant during non-blooming conditions throughout the year. Whereas high contributions by cryptophytes have been described, the observed contributions by prasinophytes are relatively novel to the region. The lack of previous observations could be due to the fact that many prasinophyte species are pico-sized and not well preserved or easy observable via microscopy, which most prior regional phytoplankton studies have relied upon (Ansotegui et al. 2003). Chemtax analysis has been shown to be particularly well suited to characterizing pico-sized prasinophytes. Specifically, many temperate coastal regions have shown high contributions by the ubiquitous, *Micromonas pusilla*, with seasonal trends similar to those of the prasinophyte group in this study (i.e., consistent presence and summer season maxima) (Not et al. 2004; Not et al. 2005;

Not et al. 2007). Fatty acid profiles have suggested that, at times, the regionally important copepod, *Neocalanus plumchrus*, supplements its diet with greater proportions of green algae which are low in essential fatty acids when compared to dinoflagellates and diatoms (El-Sabaawi et al. 2009). Therefore, the findings of this study are relevant for regional food web dynamics and have potential implications for higher trophic levels.

In line with the prevailing understanding, the statistical analyses and trends observed in this study suggest that biomass of many of the phytoplankton groups that succeeded diatom blooms (cyanobacteria, haptophytes, dictyochophytes) was driven by increased temperature, stratification, and potentially associated nutrient-depleted conditions (Harrison et al. 1983; Latasa et al. 2010; Marañón et al. 2012). Yet, the environmental drivers of the prasinophyte and cryptophyte groups remained elusive, both observationally and statistically, owing to their dynamic nature and presence across a broad range of conditions (i.e., winter through summer and nutrient-depleted to replete regimes). The observed persistence was likely a result of a complex interplay of factors and the adaptability of the species that make up the prasinophyte and cryptophyte groups. For instance, persistence across seasons may have been a result of small flagellates having competitive advantages in both highly turbulent low-light winter conditions, where their small pigment packaging makes them efficient light harvesters, and in low-nutrient summer conditions where their high surface-to-volume ratios allow for efficient nutrient uptake (Marañón et al. 2012). Both mixotrophy and osmotrophic behavior, observed in prasinophytes and cryptophytes, could have furthered their competitive advantage through these conditions by providing additional sources of energy during light and nutrient limitation (Smith and Hobson 1994; Hammer and Pitchford 2006; Unrein et al. 2007; Vargas et al. 2012; Stoeker et al. 2017; Vaillancourt et al. 2018). While dissolved organic carbon and ammonium were not measured in this study, diatom bloom degradation, freshwater influences, and high summer grazing likely provided these additional nutrient sources and may have promoted the presence of prasinophyte and cryptophyte species. Moreover, presence across seasons might have been caused by high diversity in the prasinophyte and cryptophyte groups and their ability to thrive in specific environmental niches. For example, there are multiple independent lineages or clades of *M. pusilla* that inhabit polar to tropical waters and across localized environmental gradients (Not et al. 2004; Not et al. 2005; Not et al. 2007; Foulon et al. 2008; Vaulot et al. 2008; Li et al. 2009). Finally, some pico-flagellate species have the ability to vertically migrate across the nitractine, allowing them to bloom during periods of high stratification (Rigual-Hernández et al. 2010). It is likely that these factors, coupled with top-down control as discussed below, worked to promote prasinophyte and cryptophyte contributions throughout seasons and across physical-chemical regimes.

Despite presence during eutrophic conditions, small-sized prasinophytes and cryptophytes are broadly associated with low biomass due to high grazing pressure by their microzooplankton grazers (Strom et al. 2007; Latasa et al. 2010). In the observed time series, the relative stability of prasinophyte and cryptophyte biomass through conditions ideal for growth (i.e., never reached blooming conditions despite nutrient renewal) is suggestive of this top-down control. High microzooplankton grazing has been observed historically in the NSoG supporting this argument. For instance, Haigh and Taylor (1991) observed exceptionally high summer season ciliate and heterotrophic dinoflagellate grazing with rates greater than could be supported by small phytoplankton; however, Haigh and Taylor (1991) may have missed the contributions by pico-prasinophytes found here. Comparable trends have been observed in other regions such as the Gulf of Alaska where nearly all small ($< 5 \mu\text{m}$) phytoplankton are consumed by microzooplankton resulting in low and invariable biomass (Strom et al. 2007). In turn, trophic interactions between mesozooplankton and microzooplankton may explain some of the observed interannual (i.e., higher 2018 spring season flagellate biomass) and sub-seasonal differences in prasinophyte and cryptophyte dynamics. At station QU39, Mahara et al. (2019) observed summer increases in omnivorous and carnivorous mesozooplankton communities, which would have increased grazing on the microzooplankton regulating prasinophyte and cryptophyte biomass. Further research on these trophic interactions is necessary to elucidate the complex and variable conditions observed over the summer seasons of this time series.

Chemtax Uncertainties

Chemtax pigment-based biomass estimates have been shown to provide valuable insight into phytoplankton compositions not achievable via other methods. Yet, differentiation of phytoplankton groups can be difficult in complex environments where species with similar, and varying, pigment profiles co-exist (Lewitus et al. 2005). In this study, the greatest observed Chemtax misclassifications occurred between the haptophyte and dictyochophyte groups. Specifically, this misclassification occurred when the haptophyte, *Phaeocystis pouchetti*, was present but lacked 19HF and displayed comparatively high 19BF concentrations. With the ratios utilized in this and many other Chemtax studies, 19HF is the dominant marker pigment used to discriminate the haptophyte group. Within haptophytes in general, but specifically with *Phaeocystis* spp., fucoxanthin derivatives (19BF and 19HF) show great variability in both concentrations and presence/absence and this complicates their quantification via pigment methods (Antajan et al. 2004). In the absence of 19HF, Chl *c*₃ has been suggested as an alternative pigment for detecting *Phaeocystis* spp.; however, difficulties can arise when Chl *c*₃-bearing

diatoms are co-present, which was widely observed in this study (i.e., *Pseudo-nitzschia*) (Muylaert et al. 2006).

Within Chemtax studies, phytoplankton groups are user defined with the output being restricted to these groups. As a result, if species from differing groups were present, they would be included in the most similar of the defined pigment groups (Vaillancourt et al. 2018). In this study, careful consideration was taken to select the dominant and most prevalent phytoplankton groups displaying the overarching trends in the data. Yet, there were likely groups that were not included in the analysis due to their small size, low biomass, and unknown or rare presence in the studied waters. For instance, in addition to dictyochophytes, many species within the phylum, Ochrophyta, contain 19BF as a marker pigment. Pelagophytes fall into this phylum, are pico-sized, and are important in the northeast Pacific Ocean (Fujiki et al. 2009; Yang et al. 2018); however, they are not well described in the Salish Sea and may have been too small to observe via microscopy. Due to the lack of information on local ratios for both dictyochophytes and pelagophytes, it was not possible to try to separate these groups. If present, pelagophytes would have been included in the dictyochophyte group.

In summary, the studied phytoplankton compositions were dynamic and highly complex, and at times, this created difficulties in the Chemtax analysis. The development of pigment profiles for local species and strains could help to further fine-tune input pigment ratios to improve future Chemtax phytoplankton group outputs. Furthermore, advanced methods such as flow cytometry and molecular approaches could work in conjunction with pigment-based analysis to better characterize pico-eukaryote and prokaryote communities and provide insight on local species for the determination of optimized pigment ratios (Not et al. 2005; Vaulot et al. 2008). Despite these drawbacks, the use of Chemtax in this study provided considerable advantages not provided through other methods. In general, samples for Chemtax analysis are relatively easy to collect and analyze and are cost-effective allowing for high sampling resolutions and fast results. Furthermore, sample analysis is done in a consistent and reproducible manner and is thereby less influenced by analyst skill and knowledge when compared to microscopy, which has the potential to be highly inconsistent (Schlüter and Møhlenberg 2003). Most importantly and illustrated in this work, Chemtax allows for the determination of biomass contributions from small groups (i.e., prasinophytes) not quantified via other methods and which can show important contributions under low biomass conditions spanning much of the year.

Conclusions

The studied high-resolution time series represents the first regional use of Chemtax providing unique and novel

information about phytoplankton dynamics in the NSoG. Specifically, Chemtax analysis provided information on the whole phytoplankton community and was a powerful tool to investigate the trends and variability of phytoplankton groups including small species not easily quantified via microscopy. Although diatoms formed the bulk of annual phytoplankton biomass by contributing to the majority of observed blooms events, a diverse phytoplankton community was present during non-blooming conditions throughout the year. A spring bloom was observed in each year, but timing and magnitude varied widely, likely as a result of the combined influence of solar radiation and the abatement of winter wind conditions. Spring bloom termination coincided with surface layer nutrient depletion, and post-spring diatom blooms occurred following mixing induced nutrient reintroduction to the upper layer. Yet, there were exceptions to these patterns and these are key findings of the study. First, the time series biomass maximum (July 11, 2016) was dominated by the silicoflagellate, *Dictyocha* sp. rather than diatoms, and occurred during an increase in surface FWC, temperature, and stratification. Second, in each summer (most notable in 2017 and 2018), there were nutrient renewal and drawdown events observed without increases in phytoplankton, and particularly diatom, biomass. This lack of phytoplankton accumulation indicates that losses were greater than growth, suggesting high zooplankton grazing pressure during the summer. In this study, the drivers of the most persistent phytoplankton groups, prasinophytes and cryptophytes, remained elusive due to their presence across a wide variety of environmental conditions, likely as a result of the adaptive survival strategies of the species within these groups. The greatest variability and highest biomass of these groups occurred during the summer season, and this may have been a result of trophic cascades that would allow the increase of small-sized phytoplankton. Furthermore, mixotrophy and nutrient generation may have played a role. Further research is required to elucidate the environmental drivers of the summer phytoplankton community composition and its impacts on food web dynamics.

Supplementary Information The online version contains supplementary material available at <https://doi.org/10.1007/s12237-020-00858-2>.

Acknowledgments We would like to thank the Hakai Institute's field technicians, Katie Pocock, Leo Pontier, Katie Holmes, Kate Lansley, Rachel Walker, Breanna Knowles, Chris Mackenzie, Bryn Fedje, Emma Myers, Chris O'Sullivan, and Eva Jordison, for the data collection and lab processing. Microscopy work was done by Lou Hobson, whose 50 plus years of knowledge gave much information on this system. We thank Colleen Kellogg for her guidance with the statistical analysis, Brian Hunt for initiating the data collection and Keith Holmes for his help with graphics. We gratefully acknowledge the help of the anonymous reviewers, whose insight greatly improved this manuscript.

Funding Funding for this work was provided by the Hakai Institute (JDBB and JJ) and Fisheries and Oceans Canada (AP and NN).

References

- Allen, S.E., and M.A. Wolfe. 2013. Hindcast of the timing of the spring phytoplankton bloom in the Strait of Georgia, 1968–2010. *Progress in Oceanography* 115: 6–13. <https://doi.org/10.1016/j.pocean.2013.05.026>.
- Ansotegui, A., A. Sarobe, J. María Trigueros, I. Urrutxurtu, and E. Orive. 2003. Size distribution of algal pigments and phytoplankton assemblages in a coastal-estuarine environment: Contribution of small eukaryotic algae. *Journal of Plankton Research* 25 (4): 341–355. <https://doi.org/10.1093/plankt/25.4.341>.
- Antajan, E., M.J. Chrétiennot-Dinet, C. Leblanc, M.H. Daro, and C. Lancelot. 2004. 19'-hexanoyloxyfucoxanthin may not be the appropriate pigment to trace occurrence and fate of Phaeocystis: The case of *P. globosa* in Belgian coastal waters. *Journal of Sea Research* 52 (3): 165–177. <https://doi.org/10.1016/j.seares.2004.02.003>.
- Armbrecht, L., P. Petocz, L.K. Armand, and S.W. Wright. 2015. A new approach to testing the agreement of two phytoplankton quantification techniques: Microscopy and CHEMTAX. *Limnology and Oceanography: Methods* 13 (8): 425–427. <https://doi.org/10.1002/lom3.10037>.
- Bakri, T., P. Jackson, and F. Doherty. 2017. A synoptic climatology of strong along-channel winds on the Coast of British Columbia, Canada. *International Journal of Climatology* 37 (5): 2398–2412. <https://doi.org/10.1002/joc.4853>.
- Beamish, R.J., R.M. Sweeting, K.L. Lange, D.J. Noakes, D. Preikshot, and C.M. Neville. 2010. Early marine survival of Coho Salmon in the Strait of Georgia declines to very low levels. *Marine and Coastal Fisheries: Dynamics, Management and Ecosystem Science* 2 (1): 424–439. <https://doi.org/10.1577/C09-040.1>.
- Beamish, R.J., C. Neville, R. Sweeting, and K. Lange. 2012. The synchronous failure of juvenile Pacific salmon and herring production in the Strait of Georgia in 2007 and the poor return of sockeye salmon to the Fraser River in 2009. *Marine and Coastal Fisheries*. 4 (1): 403–414. <https://doi.org/10.1080/19425120.2012.676607>.
- Blanchet, G., P. Legendre, and D. Borcard. 2008. Forward selection of explanatory variables. *Ecology* 89 (9): 2623–2632. <https://doi.org/10.1890/07-0986.1>.
- Bond, N.A., M.F. Cronin, H. Freeland, and N. Mantua. 2015. Causes and impacts of the 2014 warm anomaly in the NE Pacific. *Geophysical Research Letters* 42 (9): 3414–3420. <https://doi.org/10.1002/2015GL063306>.
- Carstensen, J., R. Klais, and J.E. Cloern. 2015. Phytoplankton blooms in estuarine and coastal waters: Seasonal patterns and key species. *Estuarine, Coastal and Shelf Science* 162: 98–109. <https://doi.org/10.1016/j.ecss.2015.05.005>.
- Chandler, P.C. 2016. Sea surface temperature and salinity trends observed at lighthouses and weather buoys in British Columbia in state of the physical, biological and selected fishery resources of Pacific Canadian marine ecosystems in 2015. In: Chandler, P.C., King, S.A., and Boldt, J. (Eds.). *Canadian Technical Report of Fisheries and Aquatic Sciences*. 3266: viii + 245 p.
- Chandler, P.C. (2017). Temperature and salinity observations in the Strait of Georgia and Juan de Fuca Strait in 2016 in state of the physical, biological and selected fisheries resources of Pacific Canadian marine ecosystems in 2016. In *Canadian Technical Report of Fisheries and Aquatic Sciences*, eds. Chandler PC, King, SA, Boldt J, 3225: 243. Victoria: Fisheries & Oceans Canada Institute Ocean Sciences.
- Chandler, P. C., M.G.G. Foreman, M. Ouellet, C. Mimeault, and J. Wade. 2017. Oceanographic and environmental conditions in the Discovery Islands, British Columbia. *DFO Canadian Science Advisory Secretariat Research Document*, (071), viii + 51 p.
- Cloern, J.E., and A.D. Jassby. 2008. Complex seasonal patterns of primary producers at the land-sea interface. *Ecology Letters* 11 (12): 1294–1303. <https://doi.org/10.1111/j.1461-0248.2008.01244.x>.
- Collins, K., S.E. Allen, and R. Pawlowicz. 2009. The role of wind in determining the timing of the spring bloom in the Strait of Georgia. *Canadian Journal of Fisheries and Aquatic Sciences* 66 (9): 1597–1616. <https://doi.org/10.1139/F09-071>.
- Coupel, P., A. Matsuoka, D. Ruiz-Pino, M. Gosselin, D. Marie, J.E. Tremblay, and M. Babin. 2015. Pigment signatures of phytoplankton communities in the Beaufort Sea. *Biogeosciences* 12 (4): 991–1006. <https://doi.org/10.5194/bg-12-991-2015>.
- Daugbjerg, N., and P. Henriksen. 2001. Pigment composition and rbcL sequence data from the silicoflagellate Dictyocha speculum: A heterokont alga with pigments similar to some haptophytes. *Journal of Phycology* 37 (6): 1110–1120. <https://doi.org/10.1046/j.1529-8817.2001.01061.x>.
- El-Sabaawi, R., J.F. Dower, M. Kainz, and A. Mazumder. 2009. Interannual variability in fatty acid composition of the copepod Neocalanus plumchrus in the Strait of Georgia, British Columbia. *Marine Ecology Progress Series* 382: 151–161. <https://doi.org/10.3354/meps07915>.
- Esenkulova, S., and I. Pearsall 2017. The phytoplankton community in the Salish Sea in state of the physical, biological and selected fishery resources of Pacific Canadian marine ecosystems in 2016. In *Canadian Technical Report of Fisheries and Aquatic Sciences*, eds. Chandler PC, King SA, Boldt J, 3225: 243. Victoria: Fisheries & Oceans Canada Institute Ocean Sciences.
- Esenkulova, S., and I. Pearsall 2019. Harmful algal blooms in the Salish Sea 2018 in state of the physical, biological and selected fishery resources of Pacific Canadian marine ecosystems in 2018. In *Canadian Technical Report of Fisheries and Aquatic Sciences*, eds. Boldt JL, Leonard J, Chandler PC, 3314: 248. Victoria: Fisheries & Oceans Canada Institute Ocean Sciences.
- Evans, W., K. Pocock, A. Hare, C. Weekes, B. Hales, J. Jackson, H. Gurney-Smith, J.T. Mathis, S.R. Alin, and R.A. Feely. 2019. Marine CO₂ patterns in the northern Salish Sea. *Frontiers in Marine Science* 5: 1–18. <https://doi.org/10.3389/fmars.2018.00536>.
- Foreman, M.G.G., M. Guo, K.A. Garver, D. Stucchi, P. Chandler, D. Wan, J. Morrison, and D. Tuele. 2015. Modelling infectious hematopoietic necrosis virus dispersion from marine salmon farms in the Discovery Islands, British Columbia, Canada. *PLoS One* 10 (6): e0130951. <https://doi.org/10.1371/journal.pone.0130951>.
- Foulon, E., F. Not, F. Jalabert, T. Cariou, R. Massana, and N. Simon. 2008. Ecological niche partitioning in the picoplanktonic green alga *Micromonas pusilla*: Evidence from environmental surveys using phylogenetic probes. *Environmental Microbiology* 10 (9): 2433–2443. <https://doi.org/10.1111/j.1462-2920.2008.01673.x>.
- Fujiki, T., K. Matsumoto, M. Honda, H. Kawakami, and S. Watanabe. 2009. Phytoplankton composition in the subarctic North Pacific during the autumn of 2005. *Journal of Plankton Research* 31 (2): 179–191. <https://doi.org/10.1093/plankr/fbn108>.
- Goela, P.C., S. Danchenko, J.D. Icely, L.M. Lubian, S. Cristina, and A. Newton. 2014. Using CHEMTAX to evaluate seasonal and interannual dynamics of the phytoplankton community off the South-west coast of Portugal. *Estuarine, Coastal and Shelf Science* 151: 112–123. <https://doi.org/10.1016/j.ecss.2014.10.001>.
- Gower, J., S. King, S. Statham, R. Fox, and E. Young. 2013. The Malaspina Dragon: A newly discovered pattern of the early spring bloom in the Strait of Georgia, British Columbia, Canada. *Progress in Oceanography* 115: 181–188. <https://doi.org/10.1016/j.pocean.2013.05.024>.

- Haigh, R., and F.J.R. Taylor. 1990. Distribution of potentially harmful phytoplankton species in the northern Strait of Georgia, British Columbia. *Canadian Journal of Fisheries and Aquatic Sciences* 47 (12): 2339–2350. <https://doi.org/10.1139/f90-260>.
- Haigh, R., and F.J.R. Taylor. 1991. Mosaicism of microplankton communities in the northern Strait of Georgia, British Columbia. *Marine Biology* 110 (2): 301–314. <https://doi.org/10.1007/BF01313717>.
- Haigh, R., F.J.R. Taylor, and T.F. Sutherland. 1992. Phytoplankton ecology of Sechelt Inlet, a fjord system on the British Columbia coast. I. General features of the nano- and microplankton. *Marine Ecology Progress Series* 89 (2–3): 117–134. <https://doi.org/10.3354/meps089117>.
- Halverson, M., J. Jackson, C. Richards, H. Melling, R. Brunsting, M. Dempsey, G. Gatien, A. Hamilton, B.V.P Hunt, W. Jacob, and S. Zimmerman. 2017. Guidelines for processing RBR CTD profiles. *Canadian Technical Report of Hydrography and Ocean Sciences*. 313: iv + 38 p.
- Hammer, A.C., and J.W. Pitchford. 2006. Mixotrophy, allelopathy and the population dynamics of phagotrophic algae (cryptophytes) in the Darss Zingst Bodden estuary, southern Baltic. *Marine Ecology Progress Series* 328: 105–115. <https://doi.org/10.3354/meps328105>.
- Harrison, P.J., J.D. Fulton, F.J.R. Taylor, and T.R. Parsons. 1983. Review of the biological oceanography of the Strait of Georgia: Pelagic environment. *Canadian Journal of Fisheries and Aquatic Sciences* 40 (7): 1064–1094. <https://doi.org/10.1139/f83-129>.
- Henriksen, P., F. Knipschildt, Ø. Moestrup, and H.A. Thomsen. 1993. Autecology, life history and toxicology of the silicoflagellate Dictyocha speculum (Silicoflagellata, Dictyochophyceae). *Phycologia* 32 (1): 29–39. <https://doi.org/10.2216/i0031-8884-32-1-29-1>.
- Higgins, H.W., S.W. Wright, and L. Schlüter. 2011. Quantitative interpretation of chemotaxonomic pigment data. In *Phytoplankton pigments characterization, chemotaxonomy and applications in oceanography*, eds. Roy S. Llewellyn CA, Skarstad Egeland E, and Johnsen G, 257–313. Cambridge: University Press.
- Holm-Hansen, O., C.J. Lorenzen, R.W. Holmes, and J.D.H. Strickland. 1965. Fluorometric determination of chlorophyll. *ICES Journal of Marine Science* 30 (1): 3–15. <https://doi.org/10.1093/icesjms/30.1.3>.
- Hooker, S. B., C.S. Thomas, L. Van Heukelem, L. Schlueter, M.E. Russ, J. Ras, H. Claustre, L. Clementson, E. Canuti, J. Berthon, J. Perl, C. Nomandea, J. Cullen, M. Kienast, and J.L. Pinckney. 2005. The Fourth SeaWiFS HPLC Analysis Round-Robin Experiment (SeAHARRE-4). *NASA Tech. Memo*, 2005–21278 (August), 112pp. Retrieved on January 2, 2018 from <http://hdl.handle.net/2060/20110008482>.
- Jackson, J.M., R.E. Thomson, L.N. Brown, P.G. Willis, and G.A. Borstad. 2015. Satellite chlorophyll off the British Columbia coast, 1997–2010. *Journal of Geophysical Research* 120 (7): 4709–4728. <https://doi.org/10.1002/2014JC010496>.
- Jochem, F., and B. Babenerd. 1989. Naked Dictyocha speculum - A new type of phytoplankton bloom in the Western Baltic. *Marine Biology* 103 (3): 373–379. <https://doi.org/10.1007/BF00397272>.
- Johannessen, S.C., D. Masson, and R.W. Macdonald. 2014. Oxygen in the deep Strait of Georgia, 1951–2009: The roles of mixing, deep-water renewal, and remineralization of organic carbon. *Limnology and Oceanography* 59 (1): 211–222. <https://doi.org/10.4319/lo.2014.59.1.0211>.
- Latasá, M., R. Scharek, M. Vidal, G. Vila-Reixach, A. Gutiérrez-Rodríguez, M. Emelianov, and J.M. Gasol. 2010. Preferences of phytoplankton groups for waters of different trophic status in the northwestern Mediterranean Sea. *Marine Ecology Progress Series* 407: 27–42. <https://doi.org/10.3354/meps08559>.
- Legendre, P., and E. Gallagher. 2001. Ecologically meaningful transformations for ordination of species data. *Oecologia* 129 (2): 271–280. <https://doi.org/10.1007/s004420100716>.
- Lewitus, A.J., D.L. White, R.G. Tymowski, M.E. Geesey, S.N. Hymel, and P.A. Noble. 2005. Adapting the CHEMTAX taxonomic composition method for assessing phytoplankton in southeastern U.S. estuaries. *Estuaries* 28 (1): 160–172. <https://doi.org/10.1007/BF02732761>.
- Li, W., F.A. McLaughlin, C. Lovejoy, and E.C. Carmack. 2009. Smallest algae thrive as the Arctic Ocean freshens. *Science* <https://doi.org/10.1126/science.1179798>.
- Lohrenz, S.E., C.L. Carroll, A.D. Weidemann, and M. Tuel. 2003. Variations in phytoplankton pigments, size structure and community composition related to wind forcing and water mass properties on the North Carolina inner shelf. *Continental Shelf Research* 23 (14–15): 1447–1464. [https://doi.org/10.1016/S0278-4343\(03\)00131-6](https://doi.org/10.1016/S0278-4343(03)00131-6).
- Mackas, D.L., and P.J. Harrison. 1997. Nitrogenous nutrient sources and sinks in the Juan de Fuca Strait/Strait of Georgia/Puget Sound estuarine system: Assessing the potential for eutrophication. *Estuarine, Coastal and Shelf Science* 44 (1): 1–21. <https://doi.org/10.1006/ecss.1996.0110>.
- Mackey, M.D., D.J. Mackey, H.W. Higgins, and S.W. Wright. 1996. CHEMTAX - A program for estimating class abundances from chemical markers: application to HPLC measurements of phytoplankton. *Marine Ecology Progress Series* 144: 265–283.
- Mahara, N., E.A. Pakhomov, J.M. Jackson, and B.P. Hunt. 2019. Seasonal zooplankton development in a temperate semi-enclosed basin: Two years with different spring bloom timing. *Journal of Plankton Research* 41 (3): 309–328. <https://doi.org/10.1093/plankt/fbz016>.
- Marañón, E., P. Cermeño, M. Latasa, and R.D. Tadonléké. 2012. Temperature, resources, and phytoplankton size structure in the ocean. *Limnology and Oceanography* 57 (5): 1266–1278. <https://doi.org/10.4319/lo.2012.57.5.1266>.
- Masson, D. 2002. Deep water renewal in the Strait of Georgia. *Estuarine, Coastal and Shelf Science* 54 (1): 115–126. <https://doi.org/10.1006/ecss.2001.0833>.
- Masson, D., and P.F. Cummins. 2004. Observations and modeling of seasonal variability in the Straits of Georgia and Juan de Fuca. *Journal of Marine Research* 62 (4): 491–516. <https://doi.org/10.1357/0022240041850075>.
- Masson, D., and M.A. Peña. 2009. Chlorophyll distribution in a temperate estuary: The Strait of Georgia and Juan de Fuca Strait. *Estuarine, Coastal and Shelf Science* 82 (1): 19–28. <https://doi.org/10.1016/j.ecss.2008.12.022>.
- Mendes, C.R., C. Sá, J. Vitorino, C. Borges, V.M. Tavano Garcia, and V. Brota. 2011. Spatial distribution of phytoplankton assemblages in the Nazaré submarine canyon region (Portugal): HPLC-CHEMTAX approach. *Journal of Marine Systems* 87 (1): 90–101. <https://doi.org/10.1016/j.jmarsys.2011.03.005>.
- Moore, C.M., M.M. Mills, K.R. Arrigo, I. Berman-Frank, L. Bopp, P.W. Boyd, E.D. Galbraith, R.J. Geider, C. Guieu, S.L. Jaccard, T.D. Jickells, J. La Roche, T.M. Lenton, N.M. Mahowald, E. Marañón, I. Marinov, J.K. Moore, T. Nakatsuka, A. Oschlies, M.A. Saito, T.F. Thingstad, A. Tsuda, and O. Ulloa. 2013. Processes and patterns of oceanic nutrient limitation. *Nature Geoscience* 6: 701–710. <https://doi.org/10.1038/ngeo1765>.
- Morán, X.A.G. 2007. Annual cycle of picophytoplankton photosynthesis and growth rates in a temperate coastal ecosystem: A major contribution to carbon fluxes. *Aquatic Microbial Ecology* 49 (3): 267–279. <https://doi.org/10.3354/ame01151>.
- Muylaert, K., R. Gonzales, M. Franck, M. Lionard, C. Van der Zee, A. Cattrijse, K. Sabbe, L. Chou, and W. Vyverman. 2006. Spatial variation in phytoplankton dynamics in the Belgian coastal zone of the North Sea studied by microscopy, HPLC-CHEMTAX and

- underway fluorescence recordings. *Journal of Sea Research* 55 (4): 253–265. <https://doi.org/10.1016/j.seares.2005.12.002>.
- Nemcek, N., M. Hennekes, I. Perry. (2019). Seasonal dynamics of the phytoplankton community in the Salish Sea from HPLC measurements 2015–2018 in state of the physical, biological and selected fishery resources of Pacific Canadian marine ecosystems in 2018. In *Canadian Technical Report of Fisheries and Aquatic Sciences*, eds. Boldt JL, Leonard J, Chandler PC, 3314: 248. Victoria: Fisheries & Oceans Canada Institute Ocean Sciences.
- Not, F., M. Latasa, D. Marie, T. Cariou, D. Vaultot, and N. Simon. 2004. A single species, *Micromonas pusilla* (Prasinophyceae), dominates the eukaryotic picoplankton in the western English Channel. *Applied and Environmental Microbiology* 70 (7): 4064–4072. <https://doi.org/10.1128/AEM.70.7.4064-4072.2004>.
- Not, F., R. Massana, M. Latasa, D. Marie, C. Colson, W. Eikrem, C. Pedrós-Alio, and N. Simon. 2005. Late summer community composition and abundance of photosynthetic picoeukaryotes in Norwegian and Barents Seas. *Limnology and Oceanography* 50 (5): 1677–1686. <https://doi.org/10.4319/lo.2005.50.5.1677>.
- Not, F., M. Zapata, Y. Pazos, E. Campaña, M. Doval, and F. Rodriguez. 2007. Size-fractionated phytoplankton diversity in the NW Iberian coast: A combination of microscopic, pigment and molecular analyses. *Aquatic Microbial Ecology* 49: 255–265. <https://doi.org/10.3354/ame01144>.
- Nunes, S., M. Latasa, J. Gasol, and M. Estrada. 2018. Seasonal and interannual variability of phytoplankton community structure in a Mediterranean coastal site. *Marine Ecology Progress Series* 592: 57–75. <https://doi.org/10.3354/meps12493>.
- Oksanen, J., F. Blanchet, M. Fiendly, R. Kindt, P. Legendre, D. McGlinn, R. Minchin, R. O'Hara, G. Simpson, P. Solymos, H. Stevens, E. Szoces, and H. Wagner. 2019. Vegan: Community ecology package. R package version 2.5-6. <https://www.r-project.org/web/packages/vegan/index.html>.
- Olson, E.M., S.E. Allen, V. Do, M. Dunphy, and D. Ianson. 2020. Assessment of nutrient supply by a tidal jet in the northern Strait of Georgia based on a biogeochemical model. *Journal of Geophysical Research, Oceans* 125: e2019JC015766. <https://doi.org/10.1029/2019JC015766>.
- Pawlowicz, R., O. Riche, and M. Halverson. 2007. The circulation and residence time of the Strait of Georgia using a simple mixing-box approach. *Atmosphere-Ocean* 45 (4): 173–193. <https://doi.org/10.3137/ao.450401>.
- Pawlowicz, R., T. Suzuki, R. Chappell, A. Ta, and S. Esenkulova. 2020. Atlas of oceanographic conditions in the Strait of Georgia (2015–2019) based on the Pacific Salmon Foundation's Citizen Science Dataset. *Canadian Technical Report of Fisheries and Aquatic Sciences* 3374: vii–116.
- Peña, M. A. and N. Nemcek. 2017. Phytoplankton in surface waters along line P and off the west coast of Vancouver Island in state of the physical, biological and selected fishery resources of Pacific Canadian marine ecosystems in 2016. In *Canadian Technical Report of Fisheries and Aquatic Sciences*, eds. Chandle, PC, King SA, Boldt JL, 3225: 243. Victoria: Fisheries & Oceans Canada Institute Ocean Sciences.
- Peña, M.A., D. Masson, and W. Callendar. 2016. Annual plankton dynamics in a coupled physical-biological model of the Strait of Georgia, British Columbia. *Progress in Oceanography* 146: 58–74. <https://doi.org/10.1016/j.pocean.2016.06.002>.
- Proshutinsky, A., R. Krishfield, M.-L. Timmermans, J. Toole, E. Carmack, F. McLaughlin, W.J. Williams, S. Zimmermann, M. Itoh, and K. Shimada. 2009. Beaufort Gyre freshwater reservoir: State and variability from observations. *Journal of Geophysical Research* 114: 1–25. <https://doi.org/10.1029/2008jc005104>.
- R Core Team. 2019. *R: A language and environment for statistical computing*. Vienna: R Foundation for Statistical Computing www.R-project.org/.
- Ramette, A. 2007. Multivariate analyses in microbial ecology. *FEMS Microbial Ecology* 62 (2): 142–160. <https://doi.org/10.1111/j.1574-6941.2007.00375.x>.
- Rigual-Hernández, A., M.A. Bárcena, S. Sierro, F.J. Flores, J.A. Hernández-Almeida, I. Sanchez-Vidal, A. Palanques, and S. Heussner. 2010. Seasonal to interannual variability and geographic distribution of the silicoflagellate fluxes in the western Mediterranean. *Marine Micropaleontology* 77 (1–2): 46–57. <https://doi.org/10.1016/j.marmicro.2010.07.003>.
- Schlüter, L., and F. Møhlenberg. 2003. Detecting presence of phytoplankton groups with non-specific pigment signatures. *Journal of Applied Phycology* 15 (6): 465–476.
- Seoane, S., A. Laza, and E. Orive. 2006. Monitoring phytoplankton assemblages in estuarine waters: The application of pigment analysis and microscopy to size-fractionated samples. *Estuarine, Coastal and Shelf Science* 67 (3): 343–354. <https://doi.org/10.1016/j.ecss.2005.10.020>.
- Simo-Matchim, A., M. Gosselin, M. Poulin, M. Ardyna, and S. Lessard. 2017. Summer and fall distribution of phytoplankton in relation to environmental variables in Labrador fjords, with special emphasis on *Phaeocystis pouchetii*. *Marine Ecology Progress Series* 572: 19–42. <https://doi.org/10.3354/meps12125>.
- Smith, P.J., and L.A. Hobson. 1994. Temporal variations in the taxonomic composition of flagellated nanoplankton in a temperate fjord. *Journal of Phycology* 30 (3): 369–375. <https://doi.org/10.1111/j.0022-3646.1994.00369.x>.
- Stoecker, D., P. Hansen, D. Caron, and A. Mitra. 2017. Mixotrophy in the marine plankton. *Annual Review of Marine Science* 9 (1): 311–335. <https://doi.org/10.1146/annurev-marine-010816-060617>.
- Strom, S.L., E.L. Macri, and M.B. Olson. 2007. Microzooplankton grazing in the coastal Gulf of Alaska: Variations in top-down control of phytoplankton. *Limnology and Oceanography* 52 (4): 1480–1494. <https://doi.org/10.4319/lo.2007.52.4.1480>.
- Suchy, K., N. Le Baron, A. Hilborn, R.I. Perry, and M. Costa. 2019. Influence of environmental drivers on spatio-temporal dynamics of satellite derived chlorophyll a in the Strait of Georgia. *Progress in Oceanography* 176: 102134. <https://doi.org/10.1016/j.pocean.2019.102134>.
- Tiselius, P., A. Belgrano, L. Andersson, and O. Lindahl. 2016. Primary productivity in a coastal ecosystem: A trophic perspective on a long-term time series. *Journal of Plankton Research* 38 (4): 1092–1102. <https://doi.org/10.1093/plankt/fbv094>.
- Unrein, F., R. Massana, L. Alonso-Sáez, and J.M. Gasol. 2007. Significant year-round effect of small mixotrophic flagellates on bacterioplankton in an oligotrophic coastal system. *Limnology and Oceanography* 52 (1): 456–469. <https://doi.org/10.4319/lo.2007.52.1.0456>.
- Utermöhl. 1958. Zur Vervolkommung der quantitativen Phytoplankton: methodik. *Mitteilungen Internationale Vereinigung für Theoretische und Angewandte Limnologie* 9: 1e38.
- Vaillancourt, R., V. Lance, and J. Marra. 2018. Phytoplankton chemotaxonomy within contiguous optical layers across the western North Atlantic Ocean and its relationship to environmental parameters. *Deep-Sea Research Part I* 139: 14–26. <https://doi.org/10.1016/j.dsr.2018.05.007>.
- Vargas, C., P. Contreras, and J. Iriarte. 2012. Relative importance of phototrophic, heterotrophic, and mixotrophic nanoflagellates in the microbial food web of a river-influenced coastal upwelling area. *Aquatic Microbial Ecology* 65 (3): 233–248. <https://doi.org/10.3354/ame01551>.
- Vaulot, D., W. Eikrem, M. Viprey, and H. Moreau. 2008. The diversity of small eukaryotic phytoplankton (<3 µm) in marine ecosystems. *FEMS Microbiology Reviews* 32 (5): 795–820. <https://doi.org/10.1111/j.1574-6976.2008.00121.x>.

- Winder, M., and U. Sommer. 2012. Phytoplankton response to a changing climate. *Hydrobiologia* 698 (1): 5–16. <https://doi.org/10.1007/s10750-012-1149-2>.
- Wright, S.W., A. Ishikawa, H.J. Marchant, A.T. Davidson, R.L. Van den Enden, and G.V. Nash. 2009. Composition and significance of picoplankton in Antarctic waters. *Polar Biology* 32 (5): 797–808. <https://doi.org/10.1007/s00300-009-0582-9>.
- Yang, B., S. Emerson, and A. Peña. 2018. The effect of the 2013–2016 high temperature anomaly in the subarctic Northeast Pacific (the “Blob”) on net community production. *Biogeosciences* 15 (21): 6747–6759. <https://doi.org/10.5194/bg-15-6747-2018>.
- Yin, K., P.J. Harrison, R.H. Goldblattl, and R.J. Beamish. 1996. Spring bloom in the central Strait of Georgia: Interactions of river discharge, winds and grazing. *Marine Ecology Progress Series* 138: 255–263.
- Zingone, A., E.J. Phlips, and P.J. Harrison. 2010. Multiscale variability of twenty-two coastal phytoplankton time series: A global scale comparison. *Estuaries and Coasts* 33 (2): 224–229. <https://doi.org/10.1007/s12237-009-9261-x>.